An experimental optical neuron

Hoppenbrouwers, J.J.L.

Award date:
1998

EINDHOVEN UNIVERSITY OF TECHNOLOGY
DEPARTMENT OF ELECTRICAL ENGINEERING

Telecommunications Technology and
Electromagnetics group

An experimental optical neuron

J.J.L. Hoppenbrouwers

Master thesis
Philips Research Laboratories
December 1997 – October 1998

Supervisors:

Philips Research
ir. E.C. Mos
dr. J.J.H.B. Schleipen

Eindhoven University of Technology
prof. ir. G.D. Khoe
dr. ir. H. de Waardt

Abstract

This thesis describes the experimental verification of a concept, named the injection seeding neuron. The conducted work is part of the Laser Neural Network project. The goal of this project is the realisation of a neural network in the optical domain by use of diode lasers.

The injection seeding neuron is a concept of a fully optical neuron. Both the inputs and the output of this neuron are defined by optical powers. In realising such a neuron, one of the requirements is a nonlinear function. In the injection seeding neuron, this function is realised by the injection of light into a semiconductor laser diode. Two longitudinal modes of the laser diode are used, with one above and one below threshold. The nonlinear function is obtained by increasing the injected power in the below-threshold mode. As a result, the below-threshold mode can start laser operation.

A crucial technique in the injection seeding neuron is injection locking or injection seeding. This technique is theoretically investigated.

The experimental setup consists of two parts. The main component of both parts is a laser diode with an external cavity. A tunable laser provides the input signal to the injection seeding neuron. The output wavelength of this tunable laser is very stable in order to achieve injection locking. The actual injection seeding neuron is formed by the so-called neuron laser. In the external cavity of this neuron laser, the applied feedback can be controlled for several longitudinal modes by use of a grating and a liquid crystal display.

The experiments successfully verify the concept of the injection seeding neuron. If the laser diode has a low pumping current, the measured nonlinear functions are in agreement with previously performed simulations. If the current is increased, different nonlinear functions are found. A variation of the injected frequency also has an effect on the shape of the nonlinearity.

Using the same experimental setup, a frequency converter is demonstrated.

It was difficult to obtain multiple, reproducible measurements due to instabilities in the setup. Therefore, it is recommended that the same experiments be carried out with an improved setup.

Contents

1 Introduction

This report describes a research project, carried out as the final part of the studies in electrical engineering. The project was conducted at Philips Research and the Electro-Optical Communications group of the Eindhoven University of Technology.
The work is part of the Laser Neural Network (LNN) project. In this project, an optical neural network is developed, with the use of laser diode technology. One of the advantages of the LNN is its possible high speed since the necessary calculations are done in the optical domain [1]. The current status of the LNN-project is that the underlying concept is theoretically described and experimentally verified [1]. Also, a setup is build that can learn certain simple logical functions such as XOR and AND [2]. Recently, more complex problems like one out of sixteen demultiplexing [3] are implemented and still, the capabilities of the LNN increase steadily.
An example of a possible application of the LNN is optical switching in a telecommunications network. In such communication networks, data can be send in packets. These packets have a header that contains routing information, like the destination address. The packets are routed to their destination by cross-connects, for which possibly the LNN can be used. In that case, the LNN should be able to read the incoming headers and send the packets to the output, as described in the header. Using the LNN would have as advantage that the optical signals don't have to be converted back to the electrical domain before routing is possible.
In the existing LNN, the sensitivity of a semiconductor laser to reflections of its own output is used. In this concept, the inputs are defined by optical transmissions. These inputs should be formed by optical powers in order to optimally profit from the advantages of the optical implementation. One way to do this is to use optical modulators that are controlled by optical signals. Another way of implementing optical powers as inputs is to use a technique called injection locking. In that case, the inputs are formed by the injection of light, coming from another semiconductor laser, into the laser diode. In the past, another graduate student has worked on this concept, called the injection seeding neuron [4]. His theoretical simulations suggest that it is possible to achieve neuron action with both optical powers as inputs and outputs. However, he encountered some difficulties in the experimental verification of these simulations. The project that is described here aims at experimentally showing fully optical neuron action in a laser diode.
Chapter 2 describes the physics behind semiconductor laser diodes. The concept of the injection seeding neuron is described in chapter 3. A crucial technique in this concept is injection seeding, which is discussed in chapter 4. The experimental setup is described in chapter 5, and in chapter 6 the results are presented. Finally, in chapter 7, conclusions are drawn and recommendations for future experiments are made.

2 Semiconductor lasers

Semiconductor laser diodes are the basic building blocks of the LNN. This chapter gives an introduction to the physics behind these devices. More detailed information on this subject can be found in various text books [5-8].

2.1 Optical gain

The basis of semiconductor lasers is a p-n heterojunction. The energy band diagram of such a junction is shown in Figure 2-1. It consists of a thin, p-type region, sandwiched between two (one p-type and one n-type) cladding layers. The two cladding layers have a higher bandgap energy. Under forward bias, the electrons and holes can move freely into the active region. Due to the difference in bandgap energy, a barrier is formed which prevents the carriers to cross this region. In this way, the carriers are confined to the active region, where the electron and hole populations can become substantial.

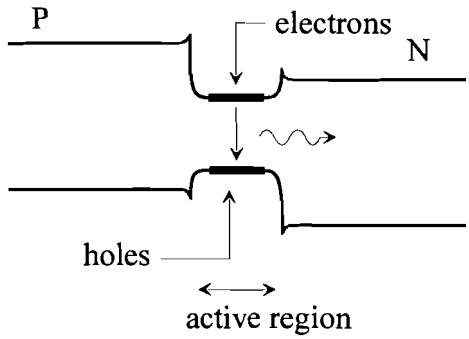

Figure 2-1: Energy band diagram of a p-n heterojunction

Electrons and holes can recombine in the active region. This recombination can be either radiatively or nonradiatively. When recombining radiatively, a photon is emitted. There are 3 types of processes involving electrons, holes and photons, which are shown in Figure 2-2. In the case of spontaneous emission a photon with random phase is emitted. A photon can also cause the emission of another photon, with the same phase and wavelength. This process is called stimulated emission. Finally, the reverse can occur and a photon is absorbed, forming a new electron-hole pair.

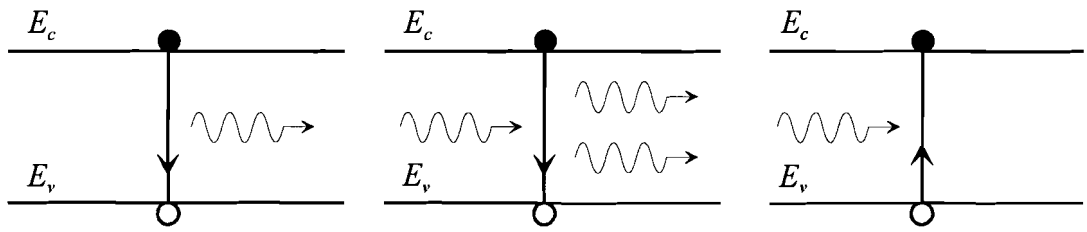

(a) spontaneous emission **(b) stimulated emission** **(c) absorption**

Figure 2-2: Processes involving electrons, holes and photons

The wavelength of the emitted light is determined by the difference between the energy levels of the electrons and holes. This energy is roughly determined by the bandgap energy, i.e. the energy difference between the valence and the conduction band. Each semiconductor material has a different bandgap energy and the emitted wave-

length of semiconductor lasers can therefore vary from a few hundred nm to a few μm.
If the electron and hole populations in the active region are high enough, the rate of stimulated photon emission will exceed that of photon absorption and the active region is said to exhibit optical gain. This regime is known as population inversion.

2.2 Fabry-Perot resonators

Optical gain alone is not enough to achieve laser operation. Another requirement is optical feedback, which is usually provided by a so-called Fabry-Perot resonator, shown in Figure 2-3.

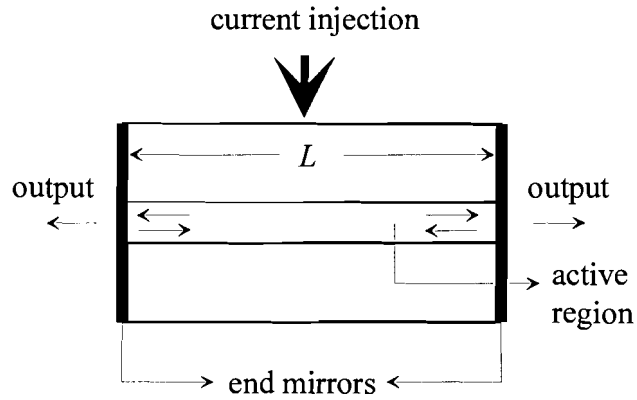

Figure 2-3: A Fabry-Perot resonator in a laser diode

The FP-cavity consists of two end planes, which partially reflect the wave that is propagating in the active region of the semiconductor laser. These end planes are formed by the semiconductor/air interface. The difference in refractive index between the semiconductor material and the surrounding air causes a (partial) reflection of the travelling wave. The reflected waves interfere with each other and this interference is only constructive for a round trip phase of 2π (or multiples). This is expressed in the well-known phase condition for the FP-cavity:

$$m\lambda = 2L, \tag{2.1}$$

with m an integer number and L the cavity length. Each value of m corresponds to a Fabry-Perot, or longitudinal, mode of the laser cavity. The laser can only start lasing at the corresponding wavelengths.
Another necessary condition to obtain laser operation is that the round-trip gain of the resonator should be equal to one. During one round-trip time through the cavity, the travelling wave experiences optical losses. These losses consist of the end mirror losses and the internal cavity losses (like absorption). Consequently, the optical gain must be high enough to compensate for these losses. Since the internal cavity losses and the gain are evenly distributed over the cavity, the roundtrip gain of the cavity can be expressed as:

$$R_1 R_2 e^{2(g-\alpha)L}, \tag{2.2}$$

with R_1 and R_2 the reflection coefficients of the cavity end-facets, g the net modal gain, α the internal losses and L the cavity length. The gain for which equation 2.2 equals unity is called the threshold gain and can be written as:

$$g_{thr} = \alpha + \frac{1}{2L}\ln\frac{1}{R_1 R_2}. \tag{2.3}$$

2.3 Gain profile and longitudinal modes

The electrons and holes that recombine to form a photon, originate from the conduction and valence band. These energy bands represent a range of energies. This implies that the emitted photons can have different wavelengths and the laser exhibits gain over a range of frequencies. The resulting gain spectrum is shown in Figure 2-4. The width of this spectrum depends on the distribution of the carriers in the energy bands. This width is typically some tens of nanometers for semiconductor lasers.

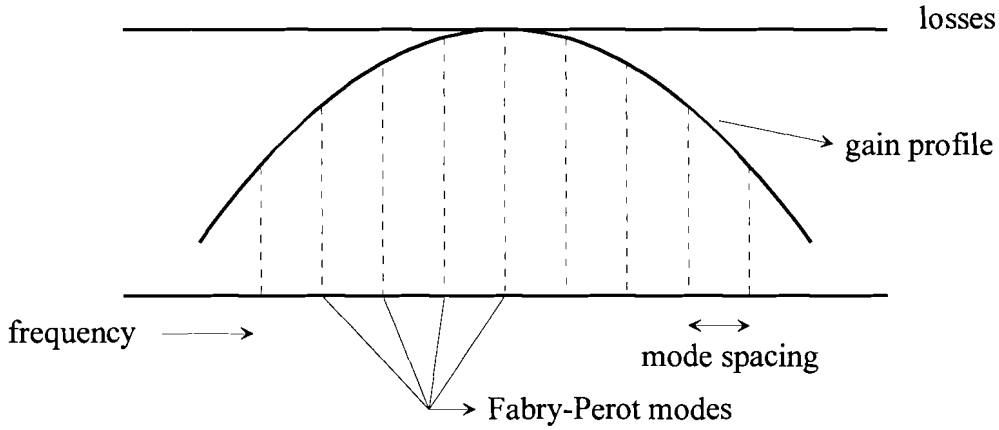

Figure 2-4: Gain-loss profile of a semiconductor laser

The Fabry-Perot cavity only permits lasing at discrete frequencies (the Fabry-Perot modes), as seen in the last section. In most lasers, the Fabry-Perot mode with the highest gain will start lasing due to an effect called mode competition [6, 9]. This effect can be explained by the fact that only a limited amount of carriers is available. The longitudinal mode that is closest to threshold (i.e. with the highest modal gain) will use most of these carriers, leaving only a small amount of gain for the other modes. For these modes, the roundtrip gain will not become equal to one (see equation 2.2) and achieving laser operation becomes very difficult.
The different Fabry-Perot modes are separated by an integer multiple of the mode spacing. The longitudinal mode-frequencies follow from equation 2.1:

$$\nu = \frac{mc}{2\mu L}, \tag{2.4}$$

with m an integer number, c the speed of light and μ the refractive index of the medium. The mode spacing is determined by:

$$\Delta\nu = \frac{c}{2\mu L}. \tag{2.5}$$

2.4 Quantum Well lasers

Carriers are confined in the active region of a p-n heterojunction. They have kinetic energies in three directions, the x,y and z direction, and their energy levels form a continuum of states. If the active layer is made sufficiently small (comparable to the de Broglie wavelength) quantum effects occur. These effects are analogous to the well-known quantum-mechanical problem of the one-dimensional potential well. As a result, the motion of the carriers in the direction normal to the active layer is quantized into discrete energy levels, which are called quantized states.
The implications for the energyband diagram are shown in Figure 2-5. The density of states function is also shown in Figure 2-5, for both the normal and the quantum well

case. It is clear that in a quantum well laser, the density of states doesn't vary continuously with the carrier energy.
These modifications of the energy distribution alter the properties of the laser. Therefore, the gain characteristics of quantum well lasers will differ from ordinary heterostructure lasers [10,11]. The number of carriers with a certain energy is limited and less than in ordinary lasers as can be seen from the density of states. This also sets a limit for the maximum gain, which doesn't depend on the pumping current. Consequently, the gain will saturate for higher currents.
It is also possible to have more than one quantum well in the active region. In this case, the laser is called a multiple quantum well laser.

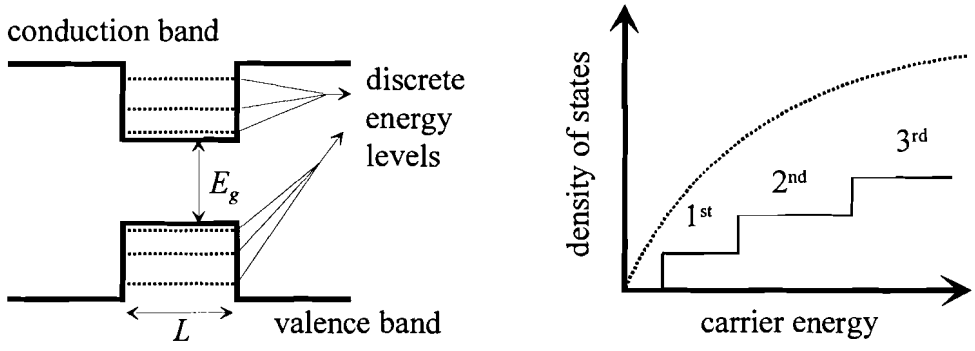

(a) Energy band diagram of a quantum well laser

(b) Density of states as function of energy
dashed: normal laser
solid: quantum well laser
three quantized states are shown

Figure 2-5: Energy bands and density of states in a quantum well laser

2.5 External cavity lasers

In the experiments, described in this thesis, lasers with an external cavity are used. Such lasers can be obtained if one of the end-facets of the laser diode is anti-reflection coated. In that case, achieving lasing operation will require very high pumping currents. If the light is reflected back into the laser from an external mirror, the laser is characterised by the external cavity instead of the (internal) active region. The resonator will now be formed by the laser end mirror that isn't anti-reflection coated and the external mirror. This is schematically shown in Figure 2-6. In order to accomplish this type of operation, the amount of residual reflection of the anti-reflection coating must be very small [12]. The amount of light, coupled back into the active region from the external cavity must be much higher than the amount of light, reflected from the anti-reflection coated facet.

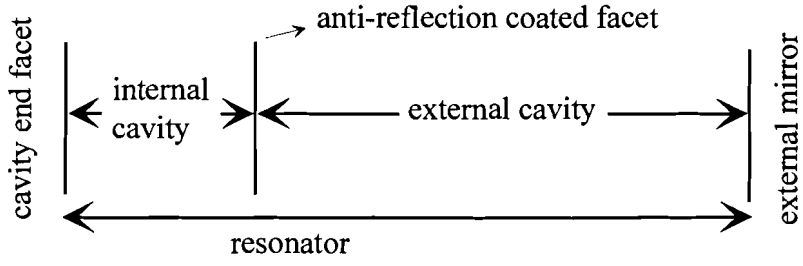

Figure 2-6: A laser diode with an external cavity

The anti-reflection coating increases the cavity losses whereas the reflection of light back into the laser cavity can be regarded as a reduction of these cavity losses. If only a part of the output spectrum is reflected back into the laser, lasing can only occur at wavelengths that are reflected. Figure 2-7 shows the gain-loss profile of an external cavity laser.
In the above-described way, the lasing wavelength can be selected. For single-mode operation, only one longitudinal mode should be reflected back into the laser. However, for long external cavity's, the mode spacing will be very small (see equation 2.5) and selecting only one longitudinal mode will be very difficult to achieve. If the reflected wavelength range is small enough, single-mode operation can occur due to mode competition and the mode with the highest modal gain will start lasing.

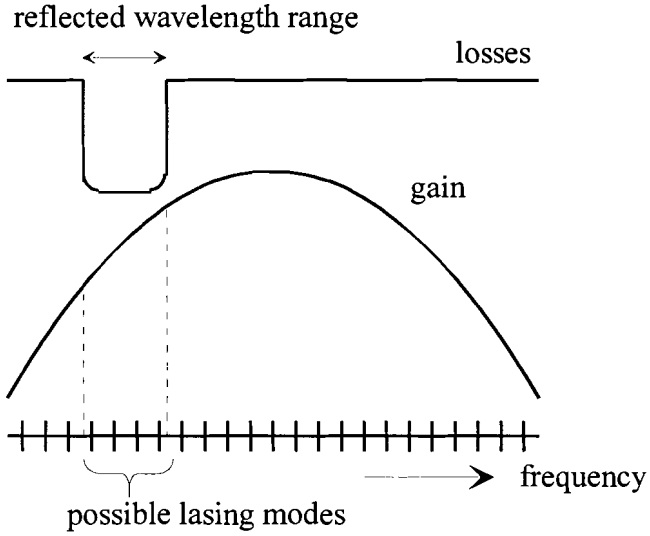

Figure 2-7: Gain-loss profile of an external cavity laser

3 Optical neural networks

This chapter describes the design of a fully optical neural network. In the first section, a short introduction to neural networks is given, followed by the description of a fully optical neuron, the so-called injection seeding neuron. Finally, an optical neural network, consisting of these neurons is described.

3.1 Introduction

Artificial neural networks operate in the same way as biological neural networks, like the human mind. They consist of a number of simple elements, called neurons. Both a biological and an artificial neuron are shown in Figure 3-1.

A biological neuron, or nerve cell, receives multiple stimuli through dendrites and synapses. If the sum of the input stimuli is high enough, the output of the neuron, the axon, will send out a stimulus itself. This output stimulus goes to another neuron or a muscle. Each input has a different influence on whether a stimulus is send or not and this influence can be positive or negative.

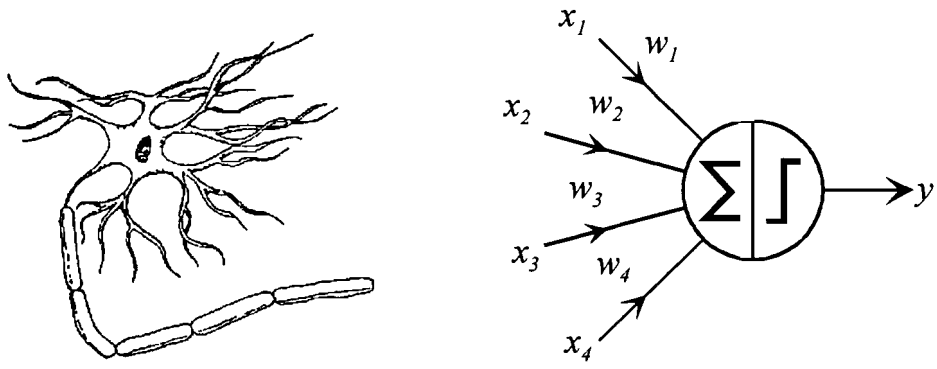

(a) biological neuron **(b) artificial neuron**

Figure 3-1: A biological and an artificial neuron

Like the biological neuron, an artificial neuron has multiple inputs. All these inputs are weighed and summed. The resulting weighed sum of inputs is compared to a threshold level. The output of the artificial neuron will become high if the weighed sum of inputs is higher than this threshold level. Accordingly, the neuron action can be described by the mathematical relation:

$$y = f(\sum_i w_i \cdot x_i), \tag{3.1}$$

with y the output, x_i the inputs, w_i the weights and f a nonlinear function, implementing the neural threshold.

Multiple neurons can be connected to form a neural network. Many different architectures of neural networks exist, and a possible example can be seen in Figure 3-2, which shows a feedforward neural network. Such a neural network has only connections in the same (forward) direction. The number of neurons and layers of such a network can be varied.

An important feature of neural networks is the fact that they can conduct many simple operations in a parallel manner. Another important aspect is their ability to learn from examples. In this way, functions with an unknown input-output relation can be trained

to the network. One way of doing this is by use of a supervised learning algorithm as described below.
The purpose of the learning algorithm is to set the weights of the neural network to values in order to obtain a certain input-output relation. The algorithm starts with setting the weights to some initial, mostly random, values. A training set is used, which contains input-output vector pairs that describe the desired function properly. The learning algorithm shows the input vectors to the network and compares the output of the network with the desired output. The algorithm calculates an error measure and the weights are adjusted depending on this error value. This is repeated iteratively until the error is within a certain limit, imposed by the learning algorithm.
After this learning process, another set of input-output vectors is shown to the network. This test set consists of vectors that aren't part of the training set. By presenting these vectors to the network, it can be verified that the network has learned the desired functionality properly.

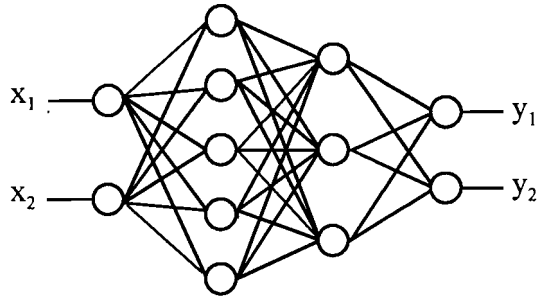

Figure 3-2: An example of a neural network

Applications of neural networking lie in the fields of pattern recognition, optimalisation and associative memories. An example of a successful application of neural networking is the prediction of the gas consumption during a day [13]. It is important for suppliers to know this consumption in advance, so they can adapt their production. The gas consumption depends on many parameters like the weather conditions, the day of the week and the hour of the day. These parameters are used as the inputs to the neural network. The network was trained with available data as the training set. In this way, the gas consumption during a day could be predicted much more precisely than before.
Neural networks are mostly implemented in software. A disadvantage of this implementation is that the parallelism is only emulated, because of the sequential nature of computers. Another option is to implement neural networks in hardware, like integrated circuits. In this way, the parallelism can be maintained but it becomes difficult to implement complex networks. The number of connections can become very high for larger neural networks, which makes the design of IC's very difficult. This will impose a limit on the complexity of the network. The disadvantages of the implementation in IC's and software aren't present when the neural network is implemented in the optical domain. In optical neural networks, the parallelism isn't emulated. An optical neural network also can support a high number of connections, since light beams can cross each other in free space without interaction.

3.2 The injection seeding neuron

3.2.1 Operation principle

An optical neural network needs optical neurons. In order to make a fully optical neural network, the neuron should have both optical inputs and outputs. This is the goal of the injection seeding neuron.

The basis of the injection seeding neuron is a semiconductor laser with optical feedback. Due to the optical feedback, the laser is lasing at a certain Fabry-Perot mode (see section 2.5), called mode 1 or the main mode. Light from an external source is injected in another Fabry-Perot mode (mode 2 or the injected mode). This can be modelled as a decrease in the optical losses at the injected wavelength.

The operation principle of the injection seeding neuron is explained in Figure 3-3. In this Figure, 3 gain-loss profiles (see Figure 2-7) are shown. For low injected powers, the decrease in the optical losses will not be sufficient to achieve laser operation in the injected mode (Figure 3-3a). For a certain level, the injected mode reaches threshold (Figure 3-3b) and both mode 1 and mode 2 will be lasing. If the injected power is further increased, the optical power will be completely switched to mode 2 and mode 1 will cease laser operation (Figure 3-3c).

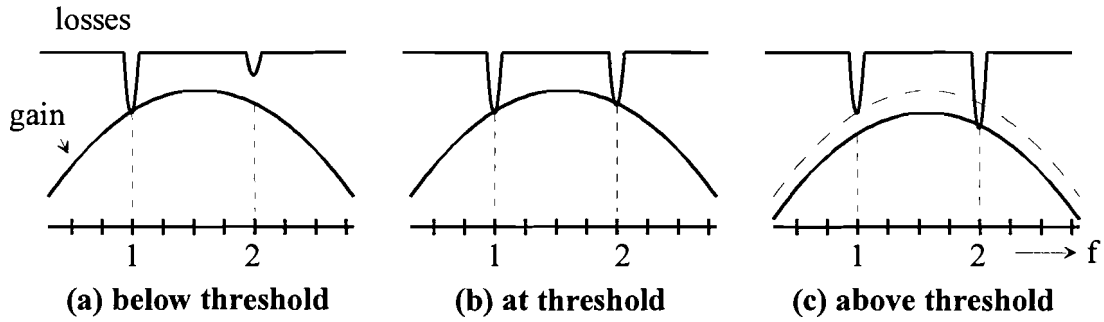

Figure 3-3: Operation principle of the injection seeding neuron

In Figure 3-4 the optical power in both Fabry-Perot modes is shown as function of the injected power in mode 2 (the regions a,b and c correspond to Figure 3-3). The result is a sigmoid, which can be used as the nonlinear function, required for neural action. In the sigmoid function, three regions can be distinguished. In region a, mode 1 is lasing and the optical powers in both modes remain constant. In region b, the optical power is switched and this is called the transition region. Finally, in region c, the optical power is completely switched to mode 2.

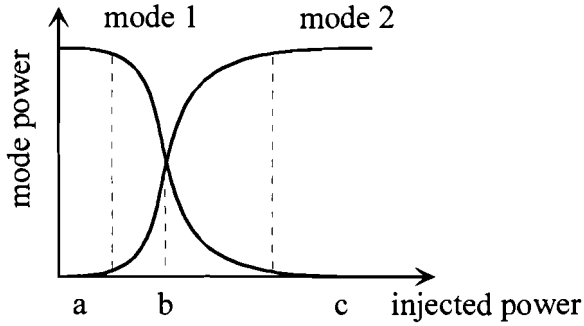

Figure 3-4: Nonlinear change in mode powers due to optical injection

If the power of the injected signal is made proportional to the weighed sum of inputs, neuron action is obtained (see equation 3.1). The optical power in the injected mode can be used as the output of the neuron.

3.2.2 Threshold variation

It is desirable to control the threshold level of the nonlinear function. For the injection seeding neuron, this can be done by changing the amount of feedback for the originally lasing Fabry-Perot mode (see Figure 3-5). If less feedback is applied, less injected power will be needed before the injected mode starts lasing. Consequently, the weighed sum of inputs needed to reach the threshold value will be lower. If the feedback is increased on the other hand, more injected power, and a higher weighed sum of inputs will be necessary to reach threshold.
Another option is adding feedback to the mode in which the power is injected. In that case, less injected power will be necessary to start laser operation in the injected mode. Accordingly, the weighed sum of inputs required to reach threshold will decrease.

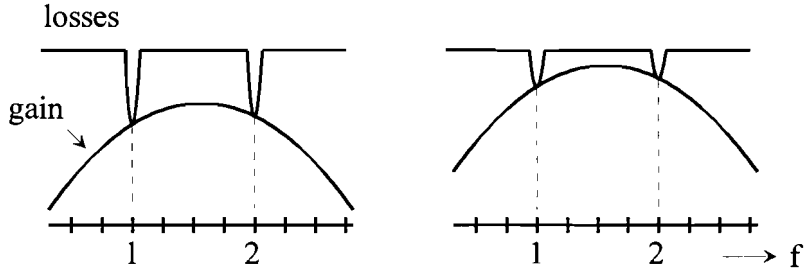

(a) initial threshold **(b) decreased threshold**

Figure 3-5: Changing the threshold by varying the applied feedback

3.3 An injection seeding neural network

3.3.1 Construction of the weighed sum of inputs

With a number of injection seeding neurons a complete neural network can be realised. However, it is still necessary to construct the weighed sum of inputs from the different input signals. This can be done by means of an optical vector matrix multiplier (see Figure 3-6). The input signals have identical wavelengths but originate from different sources. They are projected on the columns of the vector matrix multiplier. The transmission through the matrix elements of the multiplier is proportional to the corresponding weights. After this weighing, the light rays in each row are joined and the desired weighed sum of inputs is obtained. The resulting signal can be injected in an injection seeding neuron.
In the Figure, three weighed sums of inputs are constructed out of two input signals. With the appropriate vector matrix multiplier, any number of inputs and weighed sums can be supported.

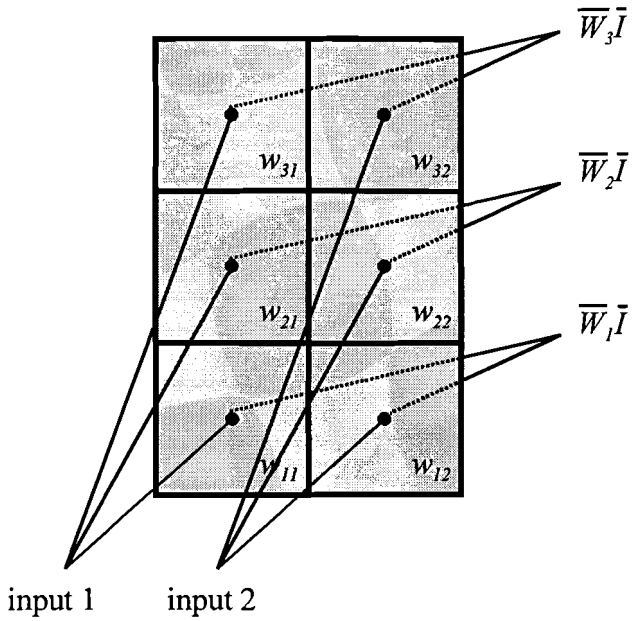

Figure 3-6: Weighing and summing by an optical vector matrix multiplier

3.3.2 Negative weights

As seen in the last section, the weights can be adjusted by varying the transmission of the matrix elements. Since this transmission can't become negative, only positive values of the weights are possible. However, some learning tasks require negative weights.

Negative weights cause the weighed sum of inputs to decrease with an increasing input signal value. The same functionality can be accomplished by increasing the threshold level of the sigmoid. As discussed earlier, this can be done by decreasing the optical losses in the main mode, which can be realised by the injection of light.

The inputs that are weighed with a positive value have an activating influence on the neuron whereas the negative weighed inputs have a deactivating influence. The activating and deactivating inputs are injected in different modes of the neuron. Therefore, the weight vector is split into two weight vectors according to the following rules:

$$w_i^+ = \begin{cases} w_i, w_i > 0 \\ 0, w_i \le 0 \end{cases} \tag{3.2}$$

$$w_i^- = \begin{cases} -1 \cdot w_i, w_i \le 0 \\ 0, w_i > 0 \end{cases} \tag{3.3}$$

With these two weight vectors, two different weighed sums of inputs (I^+ and I^-) can be formed (with x_i the input signals):

$$I^+ = \sum_i w_i^+ \cdot x_i \quad \text{and} \quad I^- = \sum_i w_i^- \cdot x_i \tag{3.4}$$

I^+ is injected at mode 2 and I^- is injected at mode 1.

This implementation of the negative weights is explained in Figure 3-7. In Figure 3-7a, only the inputs which are weighed with positive weights (I^+) are injected. The weighed sum of inputs is above threshold and the injected mode is lasing. In Figure 3-7b, the inputs that are weighed with negative weights (I^-) are injected in mode 1. This has as result that the weighed sum of inputs comes below threshold and the main mode starts lasing again.

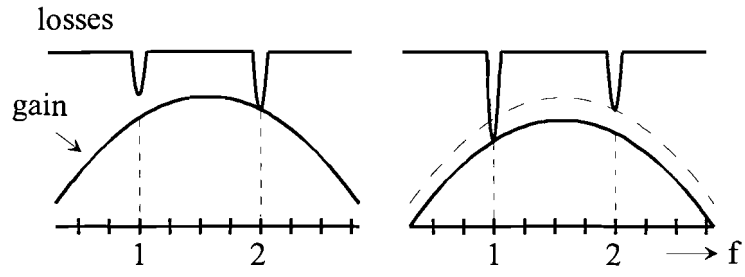

(a) injection of inputs with positive weights in mode 2

(b) injection of inputs with negative weights and positive weights

Figure 3-7: Implementation of a negative weight functionality

3.3.3 Neural network architecture

In Figure 3-8, a possible architecture of a complete neural network is shown. To obtain positive and negative weights, the input set is split. A wavelength converter makes it possible to injected the two input sets at different wavelengths. Both input sets are weighed and summed, as described in section 3.3.1. Finally, the weighed sums of inputs are injected in the injection seeding neurons.

The speed of such a neural network is expected to become comparable to the current LNN [1]. The weighing and summation won't be the limiting factor because they are done in the optical domain. The speed will be limited by the time, needed for a neuron laser to switch the output power between two modes. This mode switching can be very fast since there is no electrical charge build-up needed in this process.

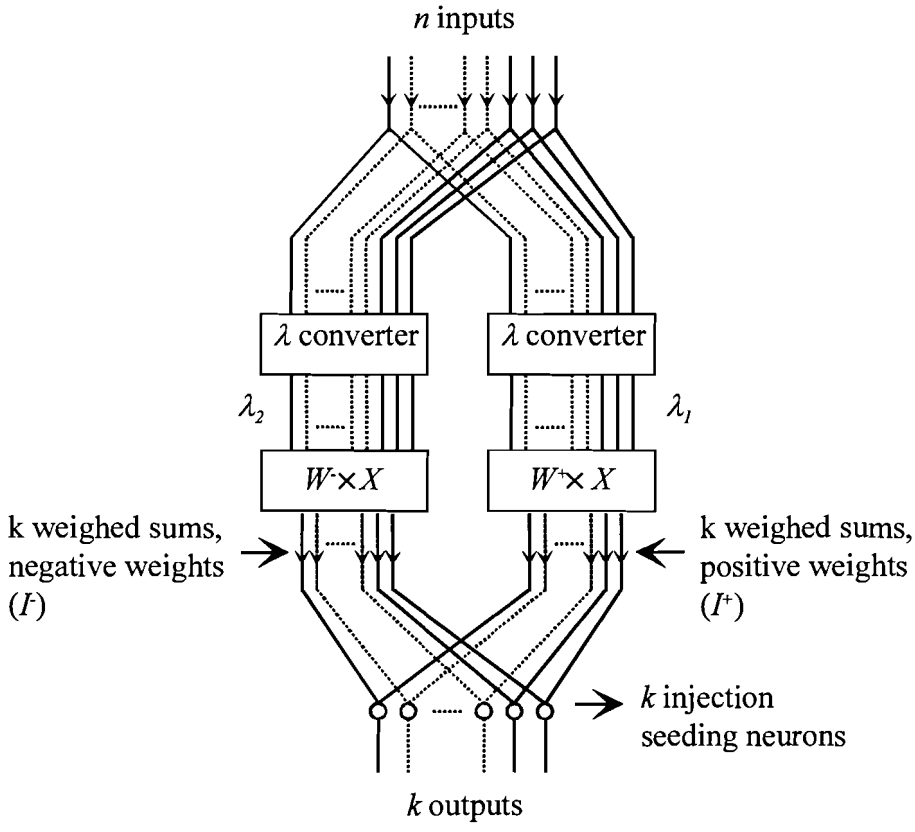

Figure 3-8: Possible architecture of an injection seeding neural network

4 Injection locking

The operation principle of the injection seeding neuron depends on a phenomenon called injection seeding or injection locking (see section 3.2.1). In this technique, light coming from a source or master laser is coupled into a second, slave laser to control its behaviour.
Injection locking is used in high-speed optical communications, for example to ensure single mode operation [14]. Another application is the synchronisation of a laser array to a master laser [15].
Two types of injection locking can be distinguished, main-mode injection locking and side-mode injection locking. In the case of main-mode injection, light is injected at a lasing mode of the slave laser. Side-mode or intermodal injection locking means that the signal is injected in a non-lasing mode of the slave laser.

4.1 Main-mode injection locking

There are several important parameters that influence the injection locking process. One of the most important is the detuning, the frequency difference between the injected signal and the lasing Fabry-Perot mode. This detuning is positive if the injected frequency is higher than the originally lasing frequency. The slave laser can only be locked to the master laser frequency when the detuning is within the so-called locking range.

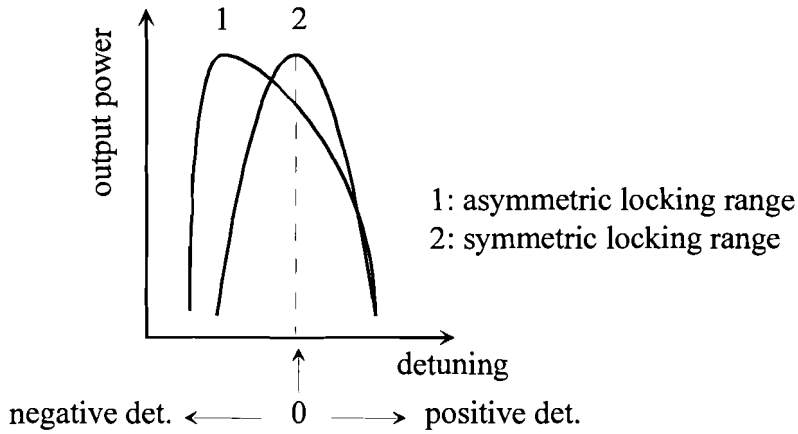

Figure 4-1: Injection locking characteristics

Intuitively, one would expect this locking range to be symmetric with respect to the detuning. In ordinary lasers (like gas lasers or dye lasers) this is true. However, this isn't the case in semiconductor lasers. For laser diodes, the locking range has a shape as shown in Figure 4-1.
From Figure 4-1, it is seen that the output power of the injected mode has a maximum for a negative value of the detuning. The cause lies in the fact that the refractive index of the active region depends on the carrier density in the active region [16]. This can be explained as follows: If injection locking is achieved, the output power of the slave laser will increase. Because this increases the recombination rate of electrons and holes, the carrier density in the active region will decrease. This will cause an increase in the refractive index of the active region and a decrease of the cavity resonance frequency (see equation 2.4). The injection locking will be optimal when the injected frequency is equal to this shifted cavity resonance frequency.
It can also be seen from Figure 4-1 that the decrease in the mode power is more rapid at the low frequency side than at the high frequency side. If the injected frequency is

higher than the optimal value, the light output will decrease. This causes an increase in the carrier density and a decrease in the refractive index. With equation 2.4, the cavity resonance frequency will increase. This will partially compensate for the detuning and the light output will decrease gradually. For an injected frequency lower than the optimal value, the cavity resonance frequency will also increase. But now, this will enhance the detuning causing a more rapid decrease of output power on this side of the locking range. The combination of these two effects causes the locking range to be asymmetric.

An analytical expression can be deduced for the locking range $\Delta\omega$ [17]:

$$-\frac{c}{2\mu_g L}\sqrt{\frac{P_i}{P}}\sqrt{1+\alpha^2} < \Delta\omega < \frac{c}{2\mu_g L}\sqrt{\frac{P_i}{P}}, \tag{4.1}$$

with P_i the number of injected photons or the injected power and P the total photon number or total power. The asymmetric nature of the locking range is expressed by α, the linewidth enhancement factor. This linewidth enhancement factor is given by:

$$\alpha = 2k_0 \frac{\partial\mu / \partial n}{\partial g / \partial n}, \tag{4.2}$$

with k_0 the wavenumber in vacuum (equals ω/c) and g the gain. The linewidth enhancement factor expresses the fact that both the refractive index and the gain are dependent on the carrier density. This dependence is only observed in semiconductor laser diodes [18].

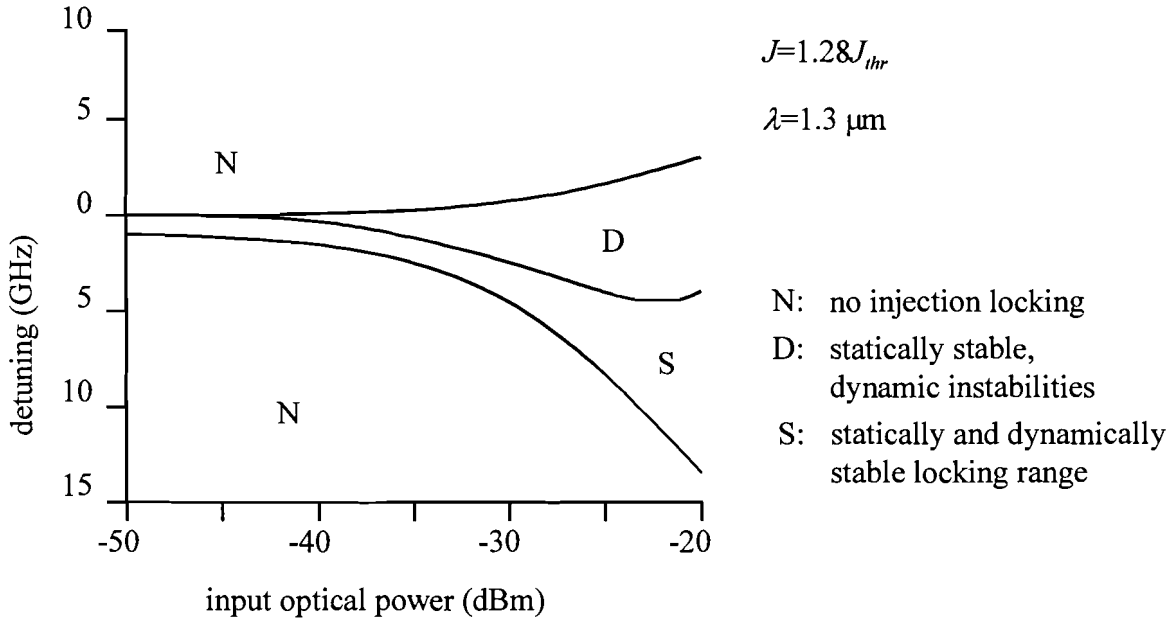

Figure 4-2: Statically and dynamically stable locking range, after [19]

The expression for the locking range, as given above, is the statically stable locking range. The laser is dynamically stable if the original, statically stable state is restored after slight perturbations. In Figure 4-2, results of numerical calculations on the locking range, as done by L. Li [19] are shown. In this Figure, the locking range is shown as a function of the injected power. For a certain injection level, instabilities start to occur and these instabilities become more profound for higher injected powers. It can also be seen that the dynamically stable locking range is smaller than the statically stable locking range. The calculations were done for an emitted wavelength of 1.3 μm

and a linewidth enhancement factor of 3.0. Mogensen et al. obtained similar results for an emitted wavelength of 830 nm [20].

4.2 Side-mode injection locking

In the case of side-mode injection locking, the signal is injected at a non-lasing Fabry-Perot mode of the laser. This means that, in order to achieve injection locking, the output power of the laser must be switched from the lasing mode, to the non-lasing, target mode. Again, there is a statically and a dynamically stable locking range, as in the case of main-mode injection locking.

Three types of operation can be distinguished [21,22]:

- Stable, single mode operation: in this case, injection locking is achieved.
- Two-signal operation: injection locking is achieved, but the injected power is not sufficient to completely switch all the power to the target mode.
- Unstable operation: the frequency of the injected signal is outside the dynamically stable locking range.

It has been found, both theoretically and experimentally, that for side-mode injection locking, the locking range is increased in comparison with main mode injection locking [22,23]. This holds for both the statically and the dynamically stable locking range. An expression, analogous to equation 4.1, can be obtained for side-mode injection locking. Note that in this case, P represents the total photon number or optical power in the injected Fabry-Perot mode.

The enhancement of the locking range is explained in Figure 4-3 [23]. For main-mode injection locking (mode m), only a small amount of injected power is sufficient to achieve injection locking. In the case of side-mode injection locking (mode s), the difference in gain between the main mode and the side mode must be compensated to reach threshold for the target mode. Therefore, a larger amount of injected power is necessary to achieve injection locking. This will increase the ratio P_i/P of equation 4.1 and consequently, the locking range will expand. Note that the locking range broadens when the side mode is chosen further away from the main mode.

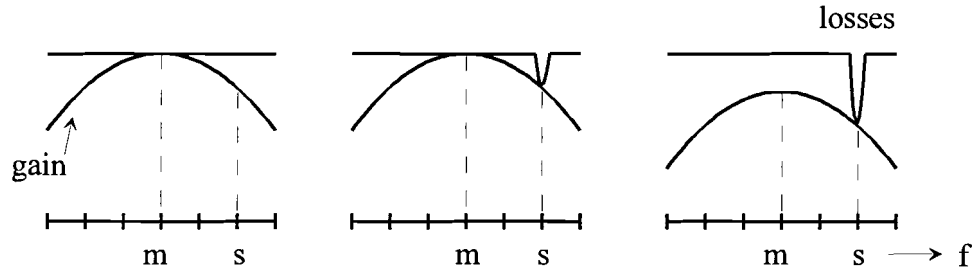

(a) no injection **(b) threshold** **(c) above threshold**

Figure 4-3: Locking range increase for side-mode injection locking

4.3 Injection locking in the injection seeding neuron

Figure 4-2 shows that the width of the locking range is a few hundred MHz. However, the calculations of reference [19] were carried out for a longitudinal mode spacing of 125 GHz. In the injection seeding neuron, an external cavity laser is used, which means that the longitudinal mode spacing will be much smaller. For example, a laser with an external cavity of 0.5 m has a mode spacing of 300 MHz (equation 2.5). This will result in a much smaller locking range, according to equation 4.1. For a linewidth

enhancement factor of 3.0 and a ratio P_i/P of 0.01, this will result in a (only statically stable) locking range of approximately 125 MHz.
In the injection seeding neuron, both main-mode injection locking and side-mode injection locking will be used. Side-mode injection locking will be used in order to obtain the nonlinear function as described in see section 3.2.1. It is stated in section 4.2 that the locking range is enhanced for side-mode injection locking. However, this enhancement is due to a large gain difference between the 2 modes. In the injection seeding neuron, one of the modes will be just above, and the other just below threshold. This means that the gain difference between the two modes will be small and there will only be a slight enhancement of the locking range.
In the implementation of the negative weight functionality (see section 3.3.2), a signal will be injected at the lasing mode of the injection seeding neuron. This is a case of main-mode injection locking.
Anyhow, it is clear that the locking range will be very small in the injection seeding neuron and it is therefore desirable to make the external cavity as small as possible.

4.4 Four-wave mixing and multi-wave mixing

If a signal is injected at a frequency outside the locking range, frequency conversion effects can occur [25,26]. One of these processes is called four-wave mixing (FWM). FWM causes a new peak to appear in the output spectrum. The frequency (ω_f) at which this new component appears is determined by the relation:

$$\omega_0 - \omega_i = \omega_f - \omega_0, \tag{4.3}$$

with ω_i the injected frequency and ω_o the frequency of the lasing Fabry-Perot mode. The output spectrum will look like Figure 4-4, with $\Delta\omega=\omega_o-\omega_i$.

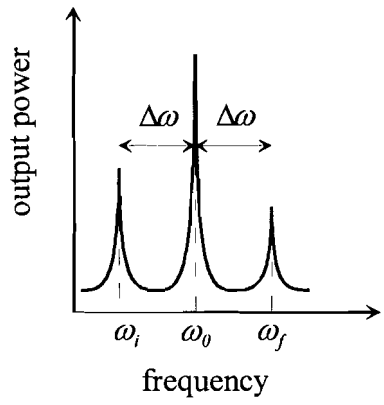

Figure 4-4: Laser spectrum in the case of four-wave mixing

Two types of FWM processes can be distinguished. If the frequency detuning between the injected and the cavity field is smaller than the cavity mode spacing, the process is called nearly degenerate FWM [27]. The process is called highly nondegenerate if the detuning is a number of times larger than the mode spacing [28]. Clearly, if the signal is injected just outside the locking range, the involved process is nearly degenerate FWM. Thus, nearly degenerate FWM will be the only process that can have an influence in the injection seeding neuron.
Nearly degenerate FWM is caused by the beating between the injected frequency and the lasing frequency. This beating induces a modulation or grating in the carrier density and the refractive index of the laser cavity [29]. The scattering of the electrical fields on this grating produces a conjugate wave at the frequency ω_f. This wave accounts for the appearance of the new component in the output spectrum.

It is also possible that higher harmonics appear in the output spectrum [29]. This can be seen as a cascade of FWM effects. The frequency difference between the frequency components in that case will always be equal to the detuning between the injected frequency and the lasing frequency.

5 The experimental setup

The experimental setup used to verify the concept of the injection seeding neuron can roughly be divided into two parts. The main component of both parts is a semiconductor laser. A tunable laser provides the input signal to the injection seeding neuron. The injection seeding neuron itself is formed by the so-called neuron laser.

5.1 The tunable laser

A laser is needed to provide the signal that is injected in the injection seeding neuron. The frequency of this signal must be adjustable, because it has to fall inside the locking range of a certain longitudinal mode (see section 4.1). An external cavity diode laser (see section 2.5) can easily achieve this tunability. There are two common configurations of such lasers, the Littrow configuration and the Littman configuration. Both use a diffraction grating as the frequency selective element. The resolution $\partial\lambda/\lambda$ of such a grating is given by the relation:

$$\frac{\partial\lambda}{\lambda} = \frac{m}{K}, \tag{5.1}$$

with m the order of the diffracted beam and K the number of illuminated grooves of the grating.

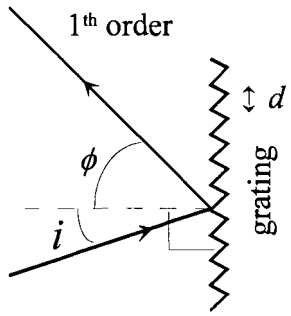

Figure 5-1: Diffraction of a light ray by a grating

The well-known grating equation describes the diffraction of the grating:

$$d(\sin i + \sin\varphi) = m\lambda, \tag{5.2}$$

with d the groove spacing of the grating, m the order of the diffracted beam, λ the wavelength, i the angle of incidence and φ the angle of reflection. Both angles are relative to the grating normal.
Using these two equations, the properties of the Littrow and the Littman configuration can be compared.

5.1.1 The Littrow configuration

The Littrow configuration is shown in Figure 5-2. A lens collimates the laser output beam and the grating diffracts the collimated light ray. A part of the first order diffraction is fed back into the laser diode. The wavelength of the reflected light is determined by the angle of the grating. In this way, the lasing wavelength can be varied if the reflected power is high enough for the laser to start lasing.
The efficiency of the grating is optimal for a horizontal polarisation of the light ray, while the light, coming from the laser has a vertical polarisation. Inserting a λ/2 plate, which rotates the polarisation, can provide polarisation matching. Another option is to rotate the laser. However, the output beam of the laser has an elliptical shape. This

means that if the laser is rotated, less lines of the grating are illuminated, resulting in a lower grating resolution (according to equation 5.1).

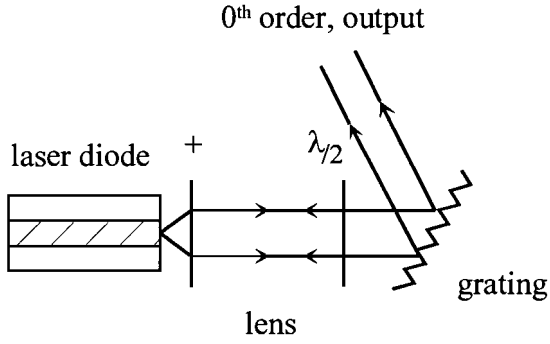

Figure 5-2: The Littrow configuration

It is clear that in the Littrow configuration, the angles of incidence and refraction at the grating are equal. In this way, we can write for i (with equation 5.2):

$$\sin i = \frac{\lambda}{2d}. \tag{5.3}$$

From this equation, we can determine the range of wavelengths, reflected back into the laser cavity:

$$\Delta\lambda = \frac{\partial\lambda}{\partial i}\Delta i = 2d\Delta i \cos i. \tag{5.4}$$

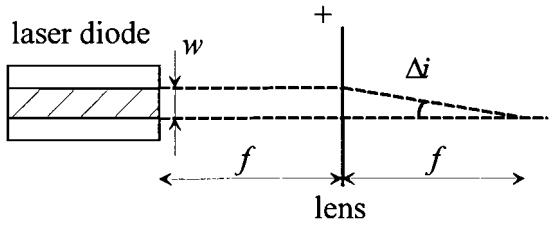

Figure 5-3: Maximum reflected angle

The maximum angle of the reflected beam that is still fed back in the active region of the laser, is restricted by the focal length of the lens (f) and the width of the active region (w) as can be seen in Figure 5-3. Since $f >> w$, $\sin\Delta i = \Delta i$ and Δi can be expressed as:

$$\Delta i = \frac{w}{f}. \tag{5.5}$$

Finally, the reflected wavelength range can be written as:

$$\Delta\lambda = \frac{2dw}{f}\cos i. \tag{5.6}$$

5.1.2 The Littman configuration

The Littman configuration [31,32] is slightly more complicated than the Littrow configuration. The cavity setup is shown in Figure 5-4. In this configuration, the 1st order diffraction is reflected back at the grating by a mirror. The wavelength can be tuned by rotating the mirror, which permits the angle of the output beam to be fixed.

If the grating is used at grazing incidence, the angle of incidence is almost 90 degrees. In this way, the grating equation (equation 5.2) can be written as:

$$\sin i = \frac{\lambda}{d}. \tag{5.7}$$

Analogous to the last section, the reflected wavelength range can be expressed as:

$$\Delta\lambda = \frac{dw}{f}\cos i, \tag{5.8}$$

with d,w and f as in the last section.

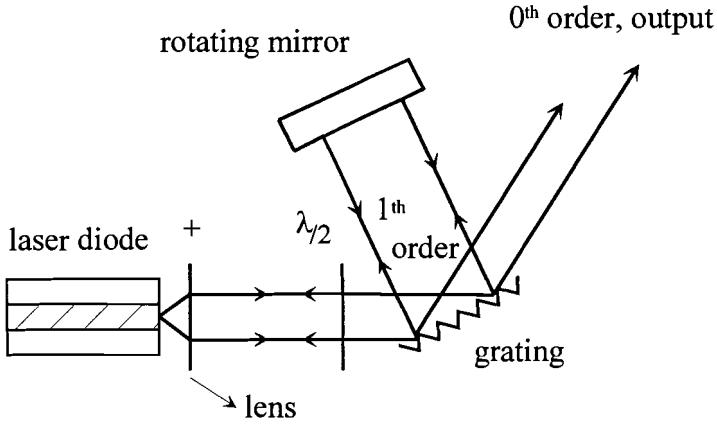

Figure 5-4: The Littman configuration

5.1.3 Littrow versus Littman configuration

To obtain single mode operation, a good wavelength selectivity and a small reflected wavelength range, $\Delta\lambda$, is necessary. If the diffraction of the Littrow and the Littman cavity are compared, it is seen that in the Littrow configuration the reflected wavelength range $\Delta\lambda$ is twice as high (according to equations 5.6 and 5.8). Furthermore, the angle of incidence i can be made close to 90° in the Littman configuration. Because the cosine of this angle is taken, the reflected wavelength range of the Littman configuration can become very low. In the Littrow configuration, this angle can't be made smaller than some tens of degrees with the available gratings. This means that in the Littman configuration, the wavelength selectivity can be made much better than in the Littrow configuration.

Another advantage of the Littman configuration is that because of the grazing incidence, more lines of the grating are illuminated. This results in a better grating resolution (equation 5.1) than in the case of the Littrow configuration.

In the Littman configuration, there are more optical elements placed in the cavity than in the Littrow configuration. This means that the optical losses in the Littman mount will be higher, and the available amount of output power will be lower than in the case of the Littrow configuration.

Finally, the angle of the 0th order reflection of the grating is fixed in the Littman configuration. This means that this beam can be used as the output of the tunable laser. If the wavelength of the laser is altered, it won't be necessary to change the alignment of the setup. If, however, the Littrow configuration were used, the angle of the 0th order reflection would change when the wavelength is altered and an extra beam-splitter should be placed in the cavity in order to provide an output beam.

In the injection seeding neuron, it is important to have a stable, single mode input signal in order to achieve injection locking (see section 4.3). The optical power of this

signal is less important. It is clear that a Littman configuration is preferred over a Littrow configuration.
The output wavelength of the tunable laser should be very stable and precisely tunable because the locking range is expected to be very small (see section 4.3). Therefore, it is decided to purchase a TEC500 tunable laser system from Sacher Lasertechnik, Marburg Germany. This is a semiconductor laser in Littman configuration. The total cavity of the laser is temperature stabilised in order to provide a stable output wavelength. The wavelength of this laser is continuously tunable between approximately 664 and 684 nm. The output power is 7.0 mW at a pumping current of 55 mA and the linewidth of a longitudinal mode is smaller than 5 MHz.

5.2 The neuron laser

For the injection seeding neuron, a laser diode with controllable optical feedback for several longitudinal modes is needed (see section 3.2) This laser is called the neuron laser. It should also be possible to inject light, coming from a tunable laser, into this part of the setup. This can be accomplished by use of the external cavity laser setup, as shown in Figure 5-5.

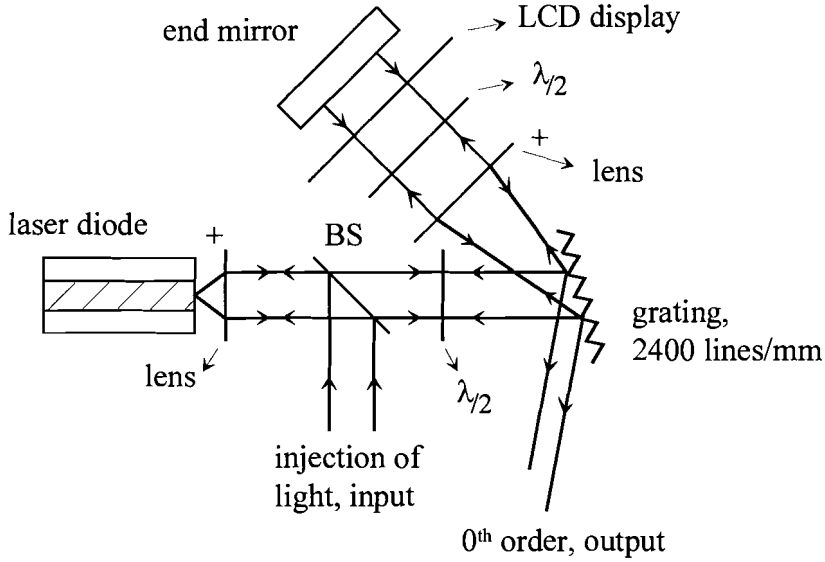

Figure 5-5: Neuron laser setup

Controllable feedback is applied to a laser diode for several modes by use of a diffraction grating, a LCD (Liquid Crystal Display) and a mirror. Light can be injected in the setup via a 70/30 beamsplitter.
The laser, used in these experiments is a multiple quantum well laser with a nominal wavelength of 680 nm (Philips Optoelectronics CQL-80X series). One side of the laser is anti-reflection coated and the residual reflectivity is less than 1%. The laser is temperature stabilised by a Peltier element to prevent thermal drift of the laser modes.
After the beam splitter, a diffraction grating separates the longitudinal modes. The 0^{th} order diffraction of the grating is used as the output beam of the injection seeding neuron. The part of the setup in which the feedback is controlled for a number of longitudinal modes is shown in more detail in Figure 5-6.

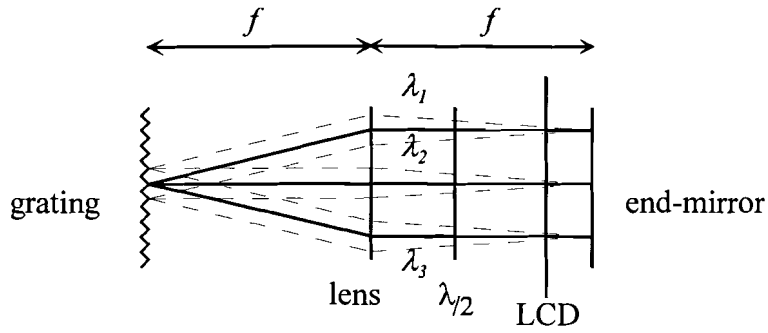

Figure 5-6: Longitudinal mode separation in the neuron laser

In the Figure, three beams are shown, corresponding to three different wavelengths. The lens compensates the angular diffraction of the grating. Each beam has a focus in the focal plane of the lens. The end-mirror is placed in this focal plane. The diffraction angle determines the position where the focus of a beam falls on the mirror. This diffraction angle is different for each wavelength and thus, the light is separated in wavelength at the cavity end mirror. The distance between the grating and the lens is made equal to the focal length of the lens, in order to ensure that the reflected beams are correctly fed back into the semiconductor laser. In the above-described way, the different longitudinal modes are spatially separated.

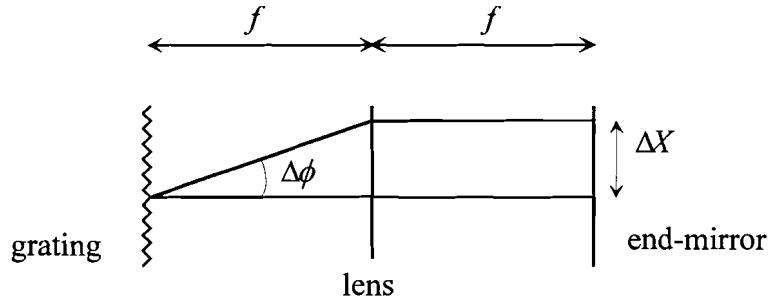

Figure 5-7: Distance between the focal points of two beams

The focal points of two beams at the end-mirror are separated by a distance ΔX. As can be seen in Figure 5-7, this distance is determined by the angle between these two beams $\Delta\varphi$ and the focal length of the lens f (since $f >> \Delta X$):

$$\Delta X = f \sin \Delta\varphi . \tag{5.9}$$

With equation 5.2, $\Delta\varphi$ can be expressed as function of a wavelength difference:

$$\Delta\varphi = \frac{\delta\varphi}{\delta\lambda}\Delta\lambda = \frac{m}{d\cos\varphi}\Delta\lambda . \tag{5.10}$$

A liquid crystal display (LCD) is used to control the amount of power, reflected back into the laser. In this setup, a LCD from Cambridge Research & Instrumentation Inc., the SLM-128 spatial light modulator, is used. This LCD consists of 120 lines and each line can be driven by a different voltage through a LCD driver. The voltage that is applied to a line induces a rotation of the polarisation state of the incoming light. A polariser is attached to the LCD, which only transmits light of a certain polarisation. The combination of the polarisation rotation and the polariser transmittance allows us to control the amount of power that is fed back into the laser diode. Since this can be done for each line independently, the amount of feedback for different longitudinal modes can be controlled separately. A λ/2 plate is inserted between the grating and

the LCD display, because the LCD works best for a certain polarisation of the incoming light, which is different from the optimal polarisation for the grating.
In the ideal case, each external cavity mode coincides with one line of the LCD display. In the setup that is described here, the length of the external cavity is approximately 30 cm. A shorter external cavity isn't possible due to the physical sizes of the components. With equation 2.5, this cavity size results in a mode spacing of 500 MHz, which is equal to 0.00076 nm.
The available LCD-display has a mode pitch of 100 μm, which makes it virtually impossible to match each external cavity mode to a LCD line. Alternatively, the line pitch of the LCD display is matched with the internal cavity mode spacing of the laser diode. In this way, the mode with the highest gain will start lasing if the feedback is high enough. When an appropriate focal length of the lens is chosen (in this case, f = 8cm), it is possible to match the internal cavity mode spacing to the LCD line pitch. This can be done by rotating the grating, which is equal to changing the diffraction of the grating (see equation 5.2).

5.3 The complete experimental setup

The complete setup for the experiments on the injection seeding neuron is shown in Figure 5-8.

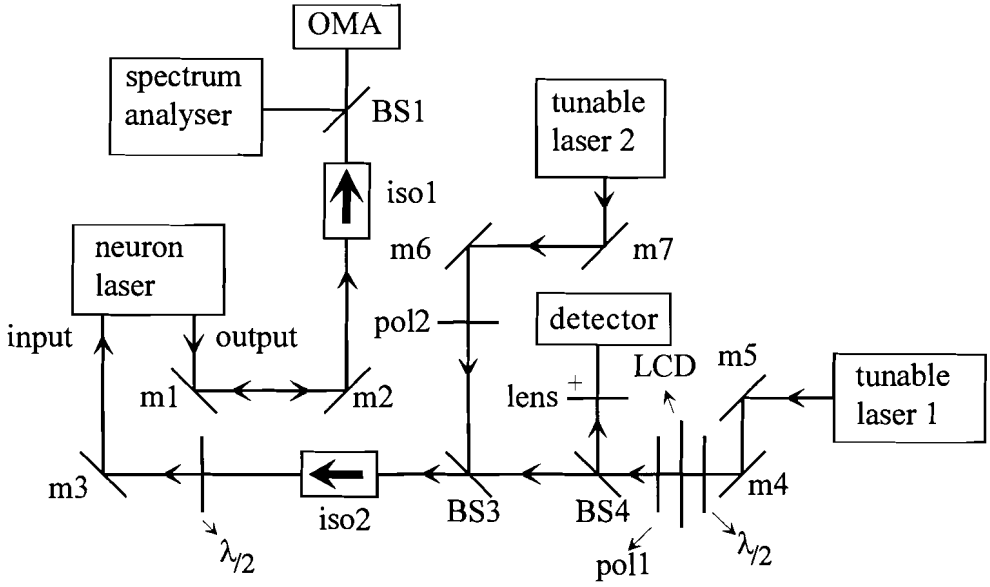

Figure 5-8: Complete experimental setup

Two tunable lasers are used in order to enable experiments on the negative weight functionality (see section 3.3). The light, coming from tunable laser 1 is amplitude modulated before it is injected in the neuron laser. This amplitude modulation is done by way of a λ/2 plate, a LCD and a polariser. The combination of these components works in the same way as described in section 5.2, except for the fact that the LCD can only be driven by one voltage. Via this voltage, the amount of power that is injected in the neuron laser can be controlled. The light from tunable laser 2 is amplitude modulated in a much simpler way, by use of a single polariser. Isolator 2 makes sure that the light, coming from the neuron laser isn't coupled into the tunable lasers. After isolator 2, another λ/2 plate is inserted because the polarisation of the light ray after the isolator isn't optimal for injection in the neuron laser.
The output spectra can be monitored in two ways, with the Optical Multichannel Analyser (OMA) and with the spectrum analyser. The OMA measures the output

spectra on a wide wavelength scale (approximately 25 nm) with a low resolution (0.025 nm). The spectrum analyser has a high resolution (7 MHz) but a very small wavelength range (1.5 GHz, equal to 0.002 nm). Isolator 1 prevents reflections from the OMA and the spectrum analyser from being reflected back into the neuron laser.
The power, coupled into the neuron laser by tunable laser 1, can be measured with a detector. The power, injected by tunable laser 2 can be measured by another detector. This detector is mobile and is used for the measurement of optical powers at various points in the setup.
All the used measuring instruments are described in more detail in Appendix A.
Both the LCD in the neuron laser and the LCD that is placed after the tunable laser can be controlled with a personal computer. Also the measuring equipment can be controlled with a personal computer. In this way, the measurements can be done automatically. Once the setup is aligned properly, only the tunable lasers have to be manually adjusted.

6 Experimental results

With the experimental setup, described in the last section, the operation principle of the injection seeding neuron is experimentally verified. First, some laser characteristics and the observed locking spectra are presented. In section 2, the nonlinear function, needed for neural action, is examined. Also, experimental results are presented on the negative weight functionality. Finally, a frequency converter, based on the same technique, is demonstrated.

6.1 Laser characteristics and locking spectra

The laser spectra can easily be obtained by coupling the output light of the laser in the OMA (see Appendix A). In Figure 6-1a, the spontaneous emission spectrum is shown. The output power of the laser can be measured with the detector (see Appendix A). If this is done for different values of the pumping current, a light-current characteristic is obtained, as shown in Figure 6-1b.

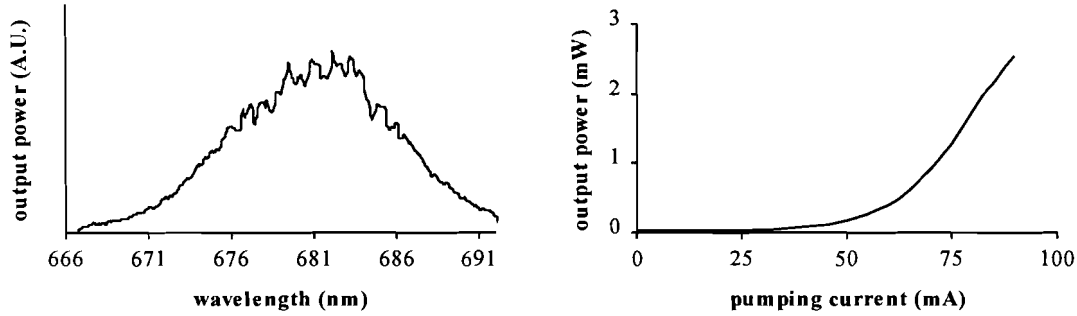

(a) (b)

Figure 6-1: Spontaneous emission and light-current characteristics

The gain-curve (see for example Figure 2-4) can be determined with the method of Gade and Osmundsen [30]. In this method, the first order reflection of a diffraction grating is coupled back into the laser diode. By rotating the grating, the tuning range can be measured. The gain profile can be obtained by plotting this tuning range for different feedback levels, which is done in Figure 6-2 for different pumping currents.

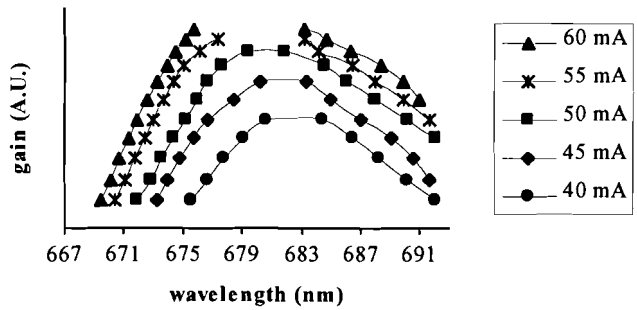

Figure 6-2: Gain profiles for different pumping currents

During the experiments on the injection seeding neuron, different locking spectra were observed. They are measured with the spectrum analyser (see Appendix A). The

locking spectra of Figure 6-3 correspond to the operation types of side-mode injection locking as described in section 4.2, namely stable locking and two signal operation. In Figure 6-3a, the injected frequency is inside the stable locking range and the signal is locked. Without the injected signal, the laser lases at another wavelength. Figure 6-3b shows two-signal operation, i.e. the signal is locked but the injected power is not sufficient to completely switch the power to the injected mode. The output power in the originally lasing mode is higher without the injected signal.

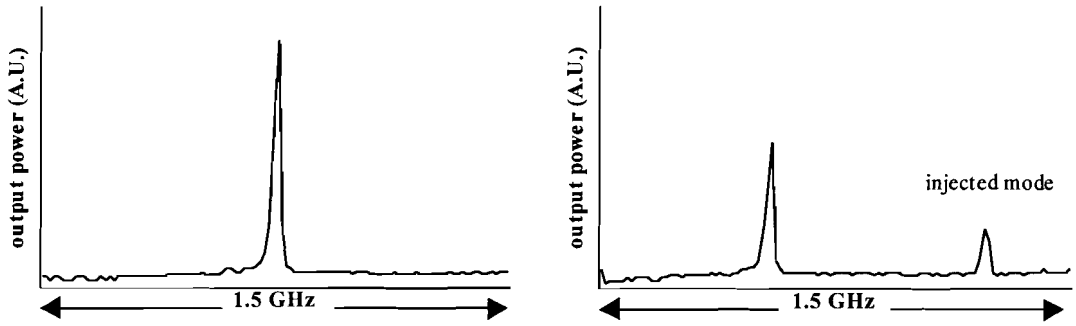

(a) (b)

Figure 6-3: Side-mode injection locking regimes

Figure 6-4 shows some frequency mixing effects (see section 4.4). These effects only occurred when the signal was injected just outside the locking range. Figure a shows a case of four-wave mixing. The originally lasing frequency is f_b. Probably, the injected frequency is f_c and the frequency formed by the four-wave mixing process is f_a. A case of multi-wave mixing is shown in Figure b. The spacing between the frequency components is equal for all components and has a value of approximately 60 MHz.

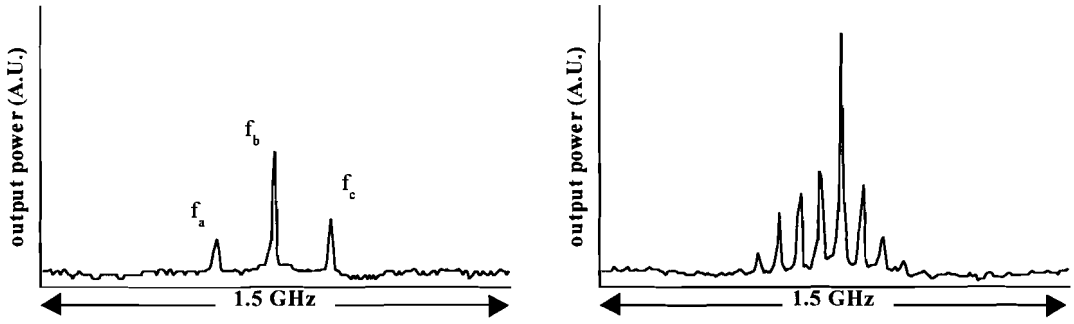

(a) (b)

Figure 6-4: Frequency mixing effects

6.2 The nonlinear function

6.2.1 Sigmoid measurements for different pumping currents

In the case of the injection seeding neuron, the nonlinear function, needed for neural action is a sigmoid (see section 3.2). It can be measured with the experimental setup of Figure 5-8 and this can be done for different pumping currents. Two longitudinal modes of the neuron laser are used. One of them is just above threshold (mode 1) and the other just below (mode 2). This is achieved by adjusting the feedback levels for both modes. The sigmoid functions are obtained by monitoring the power in both

modes with the OMA (see Appendix A) while increasing the amount of injected power in the below-threshold mode of the neuron laser. Only one of the tunable lasers of Figure 5-8 is used because there is only power injection in one longitudinal mode. During the measurements, the applied feedback for mode 1 is fixed. The feedback for mode 2 is varied to control the threshold point of the nonlinear function. The wavelength difference between the two modes is always approximately 1.5 nm (which is equal to 13 internal cavity modes). In all measurements, the modes with the highest power (i.e. with the lowest influence of the residual reflectivity of the internal cavity end-facet, see section 2.5) are used.

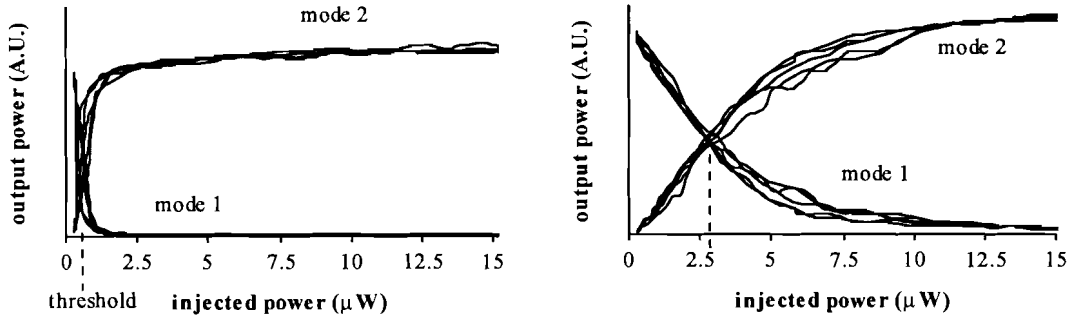

(a) (b)

Figure 6-5: Nonlinear functions for I = 60 mA

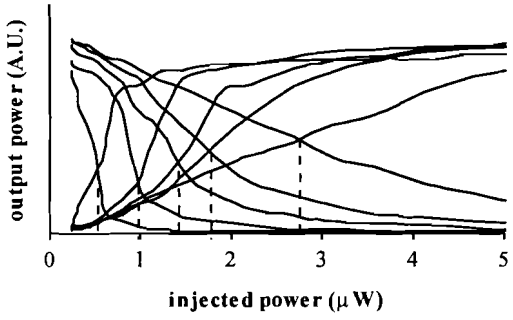

Figure 6-6: Threshold points for different feedback levels (I = 60 mA)

In Figure 6-5, results are shown for a pumping current of 60 mA. Both Figure a and Figure b show 5 measurements and the threshold points are indicated with the striped lines. The optical feedback for mode 2 was higher in the measurements corresponding to Figure a than in Figure b. As a result, less injected power is necessary to reach threshold during these measurements, as can be seen in the Figure. Figure 6-6 shows this dependency of the threshold on the feedback level in more detail. The nonlinear function is measured for 5 different values of the feedback in mode 2 and the threshold moves to higher injected powers. The size of the transition region increases for higher feedback levels. During the measurement, stable locking spectra are observed (see for example Figure 6-3). The above-described results are in good agreement with the theoretical simulations of reference [4].

Figure 6-7 shows the nonlinear function for a higher pumping current (65 mA). Again, 5 measurements are shown and the feedback for mode 2 was higher in the measurements of Figure a than in those of Figure b. Figure 6-8 shows the threshold for different feedback levels in the same way as in Figure 6-6. It is clear that the shape

of the function is modified compared to the case of a pumping current of 60 mA. For higher feedback levels, the increase of the transition region size is less.

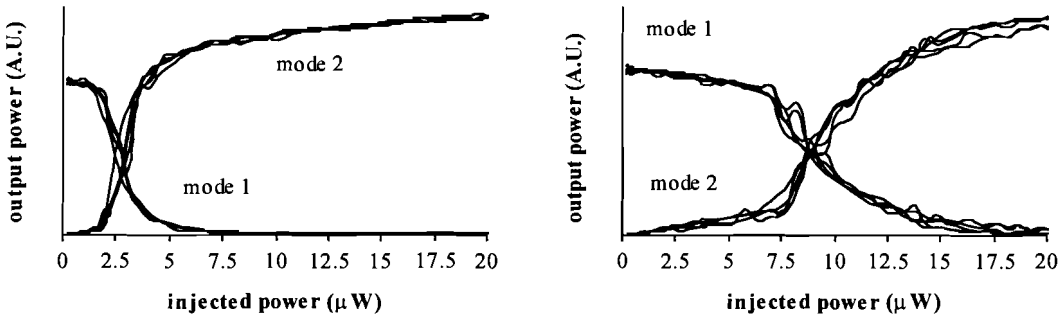

(a) (b)

Figure 6-7: Nonlinear functions for I = 65 mA

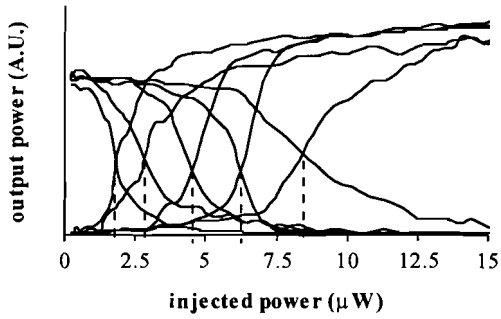

Figure 6-8: Threshold points for different feedback levels (I = 65 mA)

For still higher currents, the size of the transition region is even smaller. This can be seen in Figure 6-9, which shows measurements for a pumping current of 75 mA. Again, the feedback applied to mode 2 was lower for Figure b.
The results show that there is a spread in the threshold power for different measurements (see for example Figure 6-9).

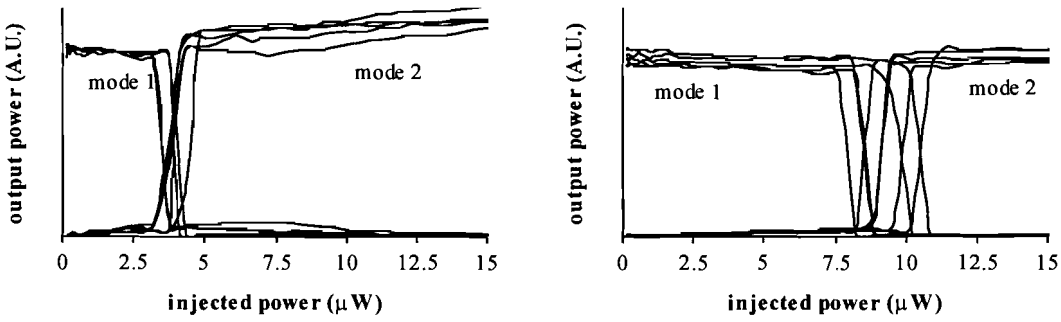

(a) (b)

Figure 6-9: Nonlinear functions for I=75 mA

The experiments indicate that a few μW's of injected power can be sufficient to totally shift the power to the below-threshold mode. In the 75 mA measurements, the output power of the laser was 6,7 mW and it was 3.5 mW in the 65 mA measurements (measured at the 0^{th} order reflection of the grating in the neuron laser).

6.2.2 Influence of the frequency of the injected signal

In Figure 6-10, the sigmoid function is shown for a high pumping current (75 mA). Mode 2 was substantially below threshold.

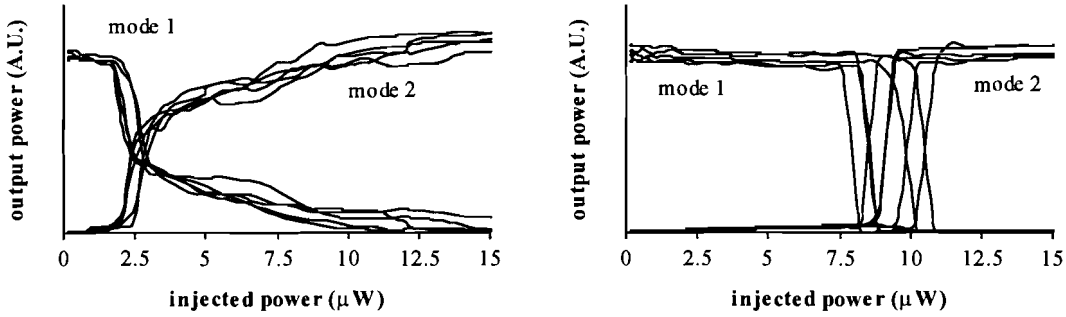

(a) (b)

Figure 6-10: Nonlinear functions for two different frequencies

The difference between Figure 6-10a and Figure 6-10b is the frequency of the injected signal. The frequency difference is a few MHz. This has an influence on both the shape and the threshold point of the sigmoid function. This effect is also present in the case of lower pumping currents, as shown in Figure 6-11 for a current of 60 mA. Again, mode 2 was substantially below threshold in this Figure.

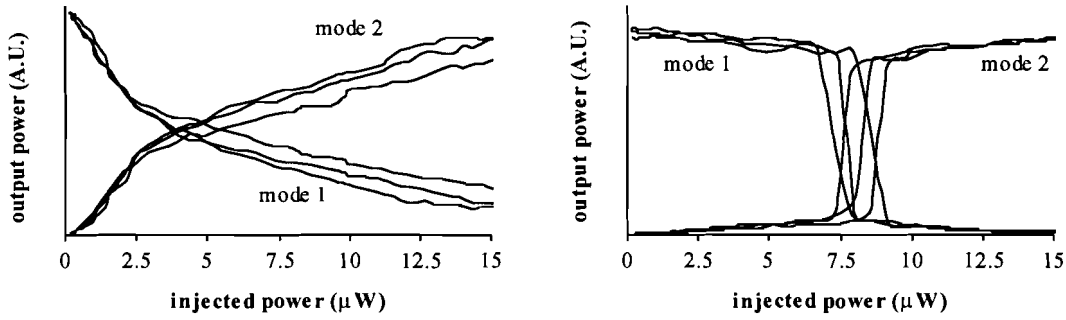

(a) (b)

Figure 6-11: Injection with different frequencies for I = 60 mA

6.2.3 Discussion

In section 6.2.1, it is seen that the shape of the sigmoid function changes for higher currents. The experimental results of that section are summarised in Figure 6-12. For lower currents (60 mA), an increase in the threshold level is accompanied by an increase in the size of the transition region. For higher currents, this isn't the case. A possible explanation for this is that the mode competition (see section 2.3) is stronger for higher currents.

The results also show a spread in the threshold point for different measurements. This effect can be explained by considering the stability of the setup. The wavelength of the light that is injected in the neuron laser by the tunable lasers is stable. This isn't the case for the longitudinal mode frequencies of the neuron laser. A small change in the external cavity length causes a drift in these mode frequencies (equation 2.4). The result is a change of the detuning between the frequency of injection and the mode frequency of the neuron laser.

Figure 4-1 shows that the output power of the locked signal varies over the locking range. This means that the power in the below-threshold mode will fluctuate due to changes in the mode frequency. This can change the point at which the injected power in the below-threshold mode is high enough to start laser operation in that mode. Consequently, the threshold point of the nonlinear function is altered.
A change in the cavity length can for example be caused by a temperature change of the optical table. During former experiments on the injection seeding neuron [4], such a temperature change was enough to shift the injected frequency out of the locking range. In those experiments, the external cavity length was approximately 1.5 m. The setup used in these experiments is much more stable thanks to the shorter cavity length of approximately 35 cm, but the drift in the cavity length will still be present.

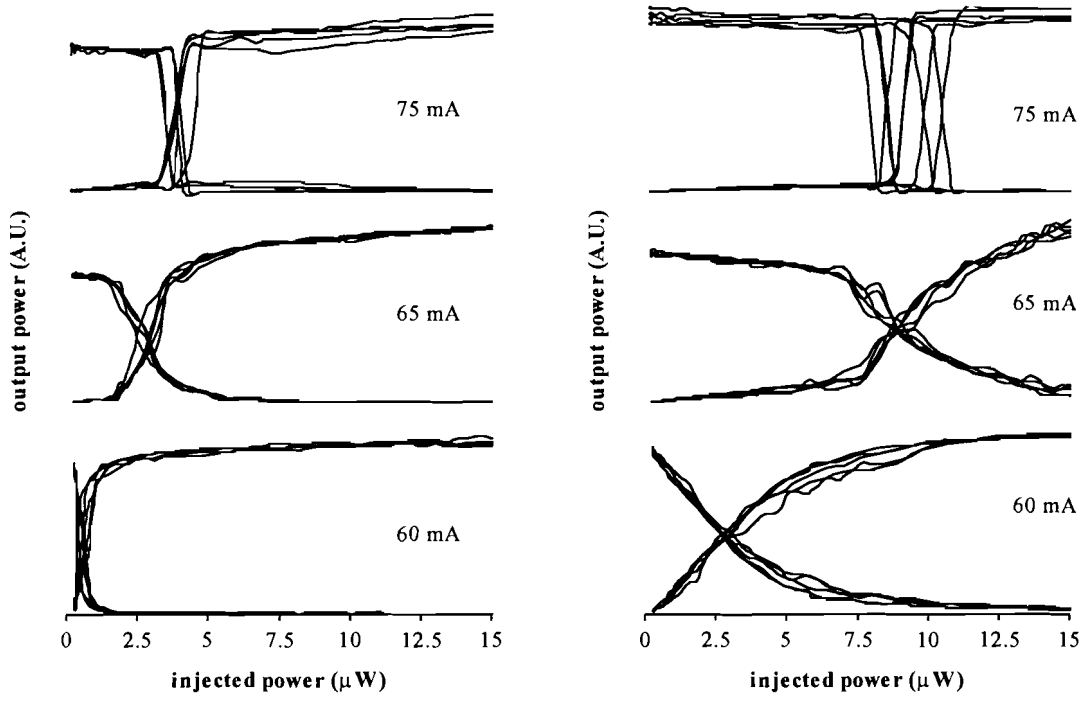

a) low threshold **(b) high threshold**

Figure 6-12: Sigmoids for different currents and feedback levels

The observed influence of the frequency of injection on the nonlinear function, as presented in Figure 6-10 and Figure 6-11, can be explained if we look at the shape of the locking range. Figure 6-13 shows the locking range of Figure 4-2 [19]. Also, two different injected frequencies and their location compared to the locking range are shown.
At frequency f_a, the locking range is reached for a low value of the injected power. This can be the case for Figure 6-11a, Figure 6-5 and Figure 6-6. In these measurements, the longitudinal mode powers are changed by the power injection right from the start of the measurement. This would mean that the frequency of the injected signal is inside the locking range for the entire measurement.
At frequency f_b, the locking range is reached for a higher injection level. Possibly, this is the case in Figure 6-10a. In that measurement, the influence of the injected signal is not present for injected powers up to 2.5 μW. It is possible that the frequency of the injected signal is outside the locking range until the injection level is approximately 2.5 μW. This isn't the case however, because at lower injection levels, it wasn't pos-

sible to achieve laser operation for mode 2 by adjusting the injected frequency. Another explanation is that for injection levels lower than 2.5 μW, the mode competition is too strong for mode 2 to start lasing.
In Figure 6-10b and Figure 6-11b, the sigmoid function is sharp. Here, it is possible that the locking range is reached for an injection level that is already high enough to completely switch the output power from mode 1 to mode 2.

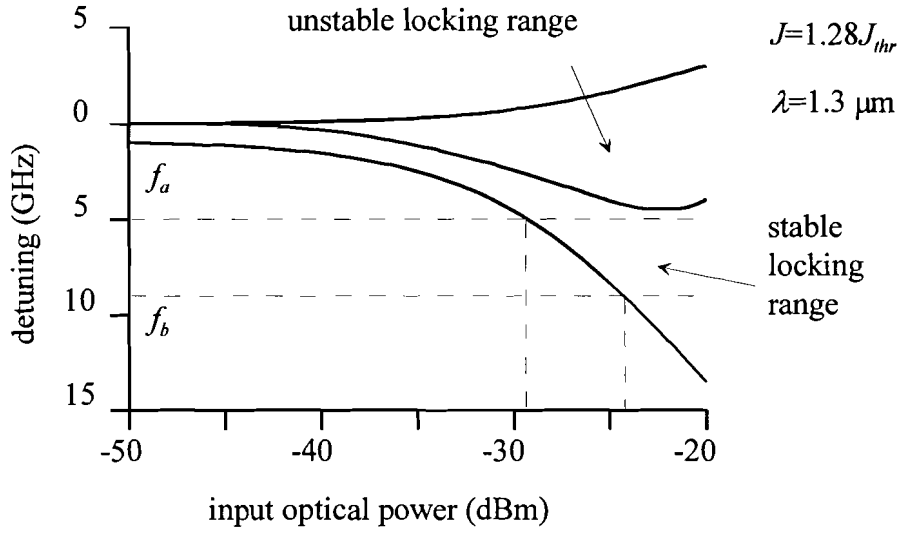

Figure 6-13: Two different injected frequencies in the locking range

6.3 Negative weights

The setup of Figure 5-8 can also be used to investigate the negative weight functionality as described in section 3.3.2. Again, two longitudinal modes of the neuron laser are used with one of them just above (mode 1) and the other just below (mode 2) threshold. This time, both tunable lasers are used because there is power injection in two modes. One tunable laser is used for power injection at a constant level, while the power, injected with the other tunable laser is gradually increased during a measurement. As in the last section, the nonlinear functions are measured by monitoring the output powers with the OMA.

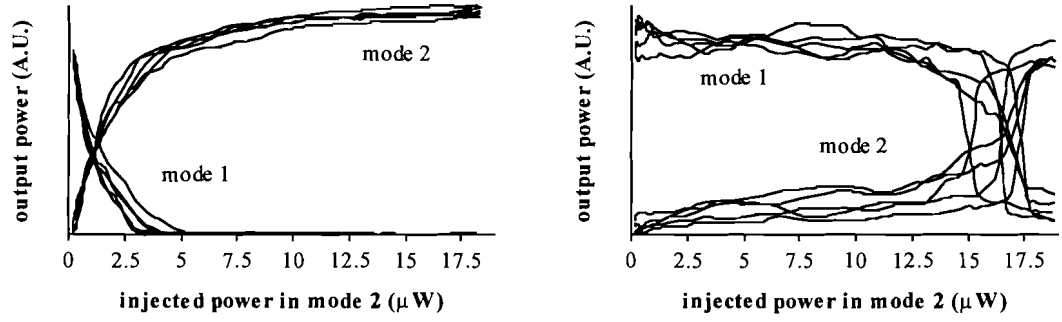

(a) $P_{inj,mode\ 1}$=0 μW (b) $P_{inj,mode\ 1}$=30 μW

Figure 6-14: Influence of power injection in mode 1 (I = 60mA)

Now, the influence of power injection in the above threshold mode (mode 1) can be determined. In Figure 6-14a, no power is injected in mode 1 and this measurement resembles the experiments described in section 6.2.1. Figure 6-14b shows the effect of

a power injection of 30 μW in mode 1 on the sigmoid function. The threshold point of the sigmoid function moves to higher injected powers. A power injection of approximately 16 μW is necessary to counteract for the power injection of 30 μW in mode 1. These values are in the same order of magnitude. The difference can be caused by a different feedback level for both modes or a different coupling efficiency for the injection of light into the laser cavity.

Figure 6-14a shows that mode 2 is lasing if there is a power injection of 10 μW in mode 2 and no power injection in mode 1. Figure 6-14B shows that if there is also power injection in mode 1 (in this case 30 μW), mode 1 is lasing for a power injection of 10 μW in mode 2. This means that if the output power in mode 2 is defined as the output power of the injection seeding neuron, the output of the neuron can be made inactive by power injection in mode 1. In this way, it is possible to deactivate the neuron and to implement weights with negative values.

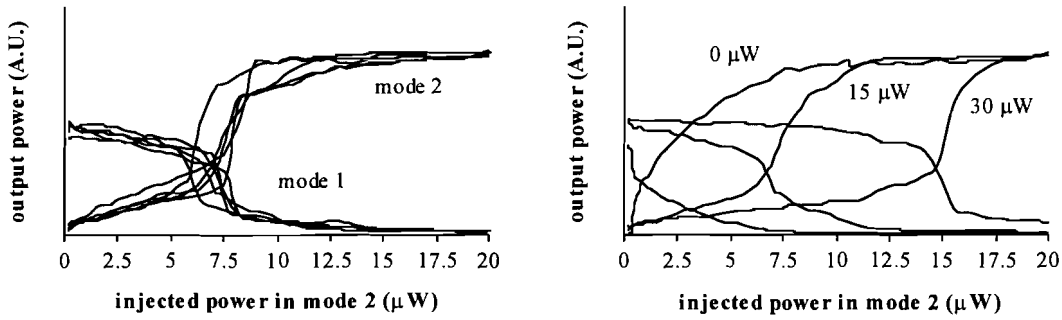

(a) $P_{inj,mode\ 1}$=15 μW **(b) threshold movement**

Figure 6-15: Variation of the injected power in mode 1 (I = 60 mA)

The threshold point of the sigmoid can be changed by altering the injected power in mode 1. Figure 6-15a shows what happens if the injected power in mode 1 is decreased to 15 μW. In Figure 6-15b, three sigmoid functions, for three different injected powers are shown. Note that a reduction of the injected power in mode 1 by a factor of 2 also halves the threshold level of the sigmoid.

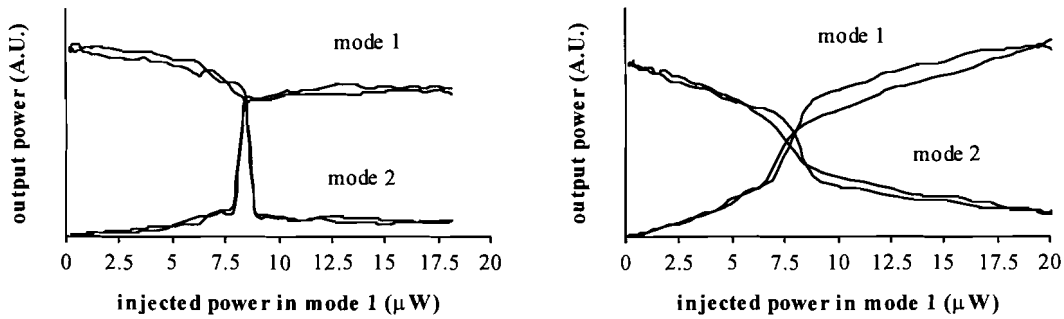

(a) **(b)**

Figure 6-16: Total mode switching with injection in two modes (I = 70mA)

The mode powers can also be totally switched from one mode to the other and back. The initially lasing mode is mode 1. This mode is switched of by the injection of power in mode 2. The injected power is kept at a constant level (in this case approximately 25 μW), which is enough for mode 2 to start lasing. Figure 6-16 shows that it

is possible to switch the output power back to mode 1 by the injection of light in this mode.

6.4 A frequency converter

The injection locking technique can also be used to demonstrate a frequency converter. Such a converter switches different incoming signals from their input wavelength to the output wavelength. It is also possible to select which inputs are converted to the output wavelength and which aren't.
The measurements, described in the last two sections, are also cases of frequency conversion. In those experiments, only 1 input wavelength is converted to the output wavelength. In the frequency converter that is demonstrated here, more input wavelengths are present.
In the frequency converter, feedback is applied to some longitudinal modes of a laser diode. Because of this feedback, one of these modes is above threshold and this mode is used as the output mode. Thus, the output is active in absence of light injection at the input modes. If a signal is injected at one of the below threshold modes, it depends on the injected power and the amount of applied feedback whether that mode will start lasing. If it starts lasing, the output mode will switch of. This means that the inverse of the input signal in converted to the output mode. Laser modes that should be converted to the output wavelength are put just below threshold. Modes that should not be converted should be far below threshold.
The setup of section 5.3 is used to demonstrate this operation principle of the frequency converter. With this setup, the feedback for 6 modes of the neuron laser is controlled. One of these modes is used as the output wavelength and the other 5 are used as the input wavelengths. Of course, any number of input wavelengths can be chosen.

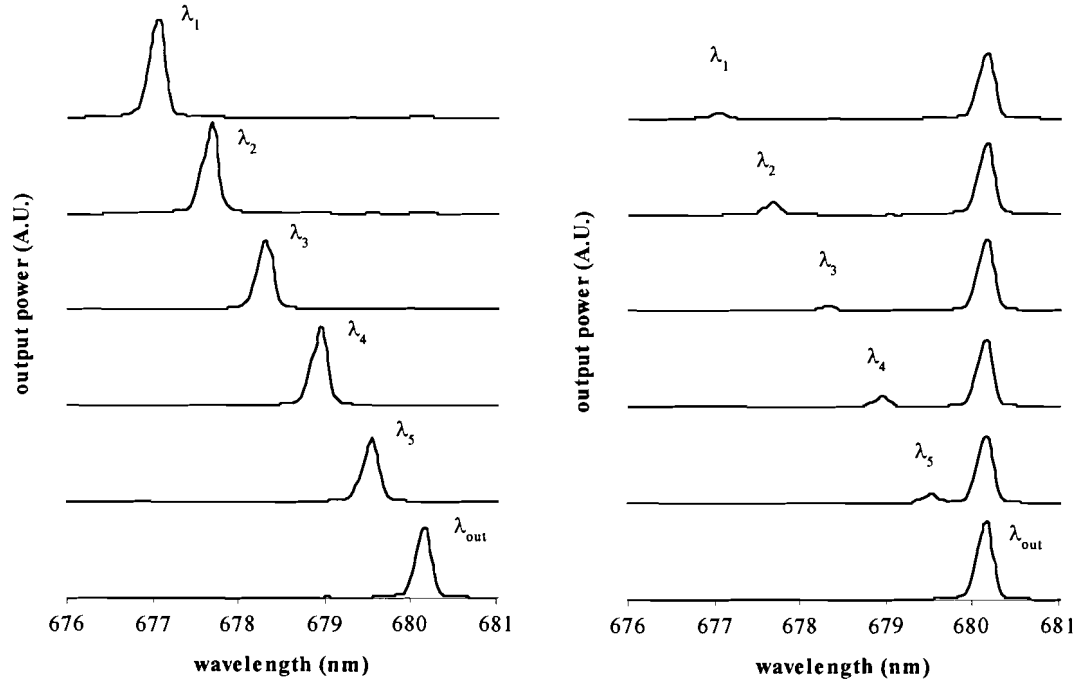

(a) inputs are converted **(b) inputs aren't converted**

Figure 6-17: Laser spectra with frequency conversion

After adjusting the feedback, the spectra of Figure 6-17 were measured by the OMA. Both Figure a and Figure b show 6 curves. For the bottom curve, there was no input signal present and the laser is lasing at the output wavelength λ_{out}. The other 5 curves correspond to the injection of light at the input wavelengths $\lambda_{1\text{-}5}$.
In Figure 6-17a, the amount of feedback was chosen in such a way that all of the injected wavelengths are converted. In Figure 6-17b none of the injected wavelengths are converted.

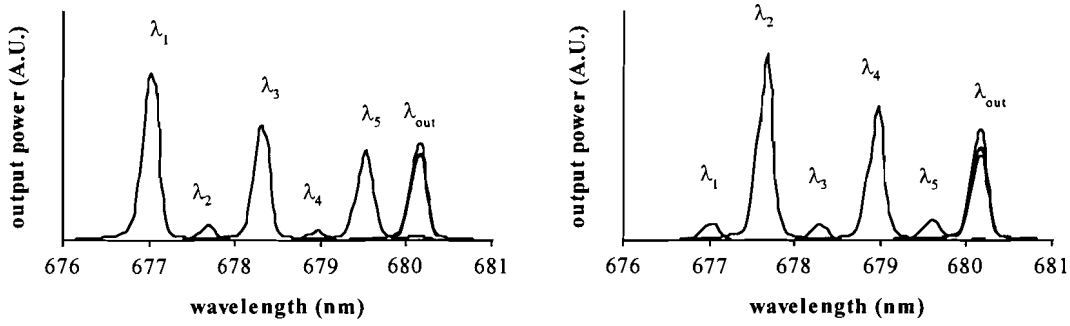

(a) (b)

Figure 6-18: Selective frequency conversion

Selective frequency conversion is shown in Figure 6-18. Now, the 6 curves are plotted superimposed. In Figure a, λ_1,λ_3 and λ_5 are converted to the output wavelength and in Figure b, only λ_2 and λ_4 are converted. In all measurements, the amount of injected power equalled 10 μW.

7 Conclusions and recommendations

7.1 Conclusions

The conducted experiments successfully verify the concept of the injection seeding neuron. It is possible to obtain a sigmoid like function and the threshold of this function can be moved by changing the amount of applied feedback for the used longitudinal modes. Therefore, this nonlinear function is suitable for neural action.
The results for low currents (60 mA) are in agreement with previously performed simulations [4]. At higher pumping currents, the slope of the sigmoid function becomes steeper than expected, which could be explained by an increase of the mode competition. The shape and the threshold point of the nonlinear function also depend on the frequency of the injected signal. This can be explained by considering the shape of the locking range.
The implementation of negative weights is also verified. The threshold of the nonlinear function can be moved by power injection in the above threshold mode and the below threshold mode of the injection seeding neuron.
Finally, the operation principle of a frequency converter is demonstrated. In this frequency converter, the wavelength of the input signals can be converted to the output wavelength. The converted wavelengths can be selected by changing the amount of applied feedback for these wavelengths.
However, it is difficult to perform multiple, reproducible measurements, especially in the experiments with the negative weight functionality. These problems are due to the small width of the locking range. As a result, an extremely stable setup is required to conduct the measurements.

7.2 Recommendations

7.2.1 Stability of the setup

It is necessary to make the experimental setup less sensitive to instabilities. The temperature drift of the optical table can cause such instabilities. The part of the setup that suffers the most of these effects is the neuron laser. A possible improvement is to place the complete neuron laser on a separate ground plate. This plate could be made of a material, such as invar that is less sensitive to temperature fluctuations than the optical table. Another option is to control the temperature of such a plate with a temperature controller and a Peltier element.
It is also possible to obtain a more stable neuron laser by minimising the length of the external cavity. This will also enhance the locking range (see equation 4.1). But with the optical elements that are currently used, a smaller cavity size isn't possible. If only 2 modes are used in the injection seeding neuron, it is possible to use an alternative setup, with a smaller external cavity (see Figure 7-1). In this setup, there is only optical feedback for two modes, supplied by two diffraction gratings. The light ray is split by a beam-splitter and the two light rays are reflected by the two gratings. The first order reflection of both gratings is coupled back into the laser diode. Actually, there are now two external cavities, each with another longitudinal mode frequency. The amount of feedback of the two modes can be controlled by the $\lambda/2$ plates, or by some other means of attenuation (for example neutral density filters). The light from the tunable lasers can be coupled in the cavity by using the 0^{th} order reflection of one of the gratings.

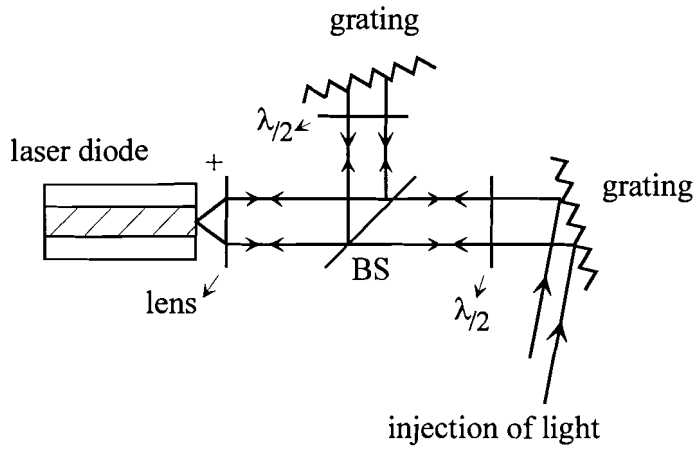

Figure 7-1: Alternative setup for the neuron laser

The length of both external cavities can be made as small as 5-7 cm. In the setup of Figure 5-5, the length of the external cavity was 37 cm. Thus, the locking range will be 6 times enhanced. This will improve the stability of the setup and consequently, the reproducibility of the measurements. Also, the influence of the injected frequency on the nonlinear function can be more accurately determined with this setup.

7.2.2 Simulations

The sigmoids as measured at low currents are predicted by simulations. There are no simulations available that confirm the effects, measured at higher currents. The simulations of reference [4] can be repeated for higher currents in order to do this.
Furthermore, the simulations of reference [4] always assume optimal detuning. Other simulations should be done to examine the influence of the frequency of injection on the nonlinear function.
With such simulations, the experimental results of this thesis can be theoretically verified. These simulations could provide a powerful instrument to predict the shape of the nonlinear function.

7.2.3 Measurements on the locking range

In section 6.2.2, it is stated that the shape of the locking range has a great influence on the sigmoid function. It is desirable to obtain an insight in the shape and width of the locking range. This can be done with the setup of Figure 7-2. The first order diffraction of the grating is coupled back into the laser. The grating is placed as close to the laser as possible in order to obtain a small external cavity (and consequently, a locking range as large as possible). The light, coming from the tunable laser can be amplitude controlled as described in section 5.3. This makes it possible to measure the width of the locking range for various injected powers and to obtain a plot of the locking range similar to Figure 4-2. Such plots can be measured for different pumping currents and for different feedback levels. The feedback levels can be controlled by inserting neutral density filters in the external cavity. If these plots of the locking range are determined, they can be used to obtain more insight in the shape of the nonlinear function.

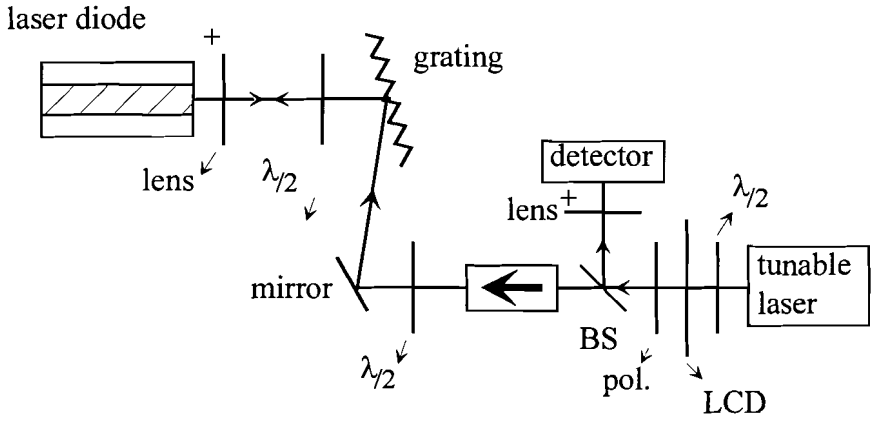

Figure 7-2: Setup for measurements on the locking range

7.2.4 A neural network with injection seeding neurons

A complete neural network needs multiple injection seeding neurons. With the current size of the setup, this would take an enormous space. Thus, it is necessary to reduce the size of the injection seeding neuron. If only two modes are used, then the setup of Figure 7-1 is a possibility, but still, complex networks with lots of neurons would have a large size. Therefore, the size of one injection seeding neuron should be minimised.

The weighed sum of inputs is constructed by adding signals from different sources (see section 3.3.1). It should be investigated whether the adding of these signals is linear. Also, the injection of such a constructed signal in the neuron laser should be examined. This should also be done for the case of injection of optical powers in two modes (like in the experiments with negative weights).

Possible applications of an injection seeding neural network lie in the field of optical telecommunications. The signals in optical communication networks usually have a higher wavelength (1.3-1.5 μm). The injection locking process should be investigated at such a wavelength.

In section 3.3.3, it was stated that the speed of operation of an injection seeding neural network can be very high. It should be investigated how high this speed can become. For this, the speed of the mode switching due to optical injection should be examined. This can be done with both simulations and experiments.

8 Bibliography

1. Colak, S.B. and J.J.H.B. Schleipen, C.T.H. Liedenbaum, *Neural network using longitudinal modes of an injection laser with external feedback*, IEEE Trans. Neural Networks, Vol 7 (1996), No 6, pp 1389-1400.
2. Mos, E.C. and J.J.H.B. Schleipen, H. de Waardt, *Optical-mode neural network by use of the nonlinear response of a laser diode to external optical feedback*, Applied Optics, Vol 36 (1997), No 26, pp 6654-6663.
3. To be published in Applied Optics.
4. Blüm, M.W., *An injection seeding neuron,* Master's thesis, Eindhoven University of Technology, The Netherlands, november 1997.
5. Agrawal, G.P. and N.K. Dutta, *Long-wavelength semiconductor lasers,* New York: Van Nostrand Reinhold, 1986.
6. K. Petermann, *Laser diode modulation and noise,* Dordrecht, The Netherlands: Kluwer Academic Publishers, 1988.
7. Neamen, D.A., *Semiconductor physics and devices: basic principles,* Homewood, IL, USA: Irwin, 1992.
8. Chuang, S.L., *Physics of optoelectronic devices.* New York: John Wiley & Sons, Inc., 1995.
9. Lee, T.-P. and C.A. Burrus, J.A. Copeland, A.G. Dentai, D. Marchuse, *Short-cavity InGaAsP injection lasers: Dependence of mode spectra and single-longitudinal-mode power on cavity length*, IEEE J. of Quantum Electronics, Vol QE-18 (1982), No 7, pp 1101-1113.
10. Mehuys, D. and L. Eng, M. Mittelstein, T.R. Chen, A. Yariv, *Ultra-broadband tunable external cavity quantum well lasers*, Proceeding of the SPIE: Laser diode technology and applications II, Vol 1219 (1990), pp 358-365.
11. Arakawa, Y. and A. Yariv, *Quantum well lasers-gain, spectra, dynamics*, IEEE J. of Quantum Electronics, Vol QE-22 (1986), No 9, pp 1887-1899.
12. Tkach, R.W. and A.R. Chraplyvy, *Regimes of feedback effects in 1,5 μm distributed feedback lasers*, IEEE J. of Lightwave Technology, Vol LT-4 (1986), pp 1655-1661.
13. Hormel, M. and C. Hausen, *Neural network based forecasting for optimal resource scheduling*, Progress in Neural Processing: Neural networks, best practice in europe, Vol 8 (1997), pp 136-141.
14. Toba, H. and Y. Kobayashi, K. Yanagimoto, H. Nagai, M. Nakahara, *Injection-locking technique applied to a 170 km transmission experiment at 445.8 Mbit/s*, Electronics Letters, Vol 20 (1984), pp 370-371.
15. Goldberg, L. and H.L. Taylor, J.F. Weller, D.R. Scifres, *Injection locking of coupled-stripe diode laser arrays*, Applied Physics Letters, Vol 46 (1985) pp 236-238.
16. Lang, R., *Injection locking properties of a semiconductor laser*, IEEE J. of Quantum Electronics, Vol QE-18 (1982), No 6, pp 976-983.

17. Petitbon, I and P. Gallion, G. Debarge, C. Chabran, *Locking bandwith and relaxation oscillations of an injection-locked semiconductor laser*, IEEE J. of Quantum Electronics, Vol QE-24 (1988), No 2, pp 148-154.

18. Osinski, M. and J. Buus, *Linewidth broadening factor in semiconductor lasers-an overview*, IEEE J. of Quantum Electronics, Vol QE-23 (1987), No 1, pp 9-29.

19. Li, L., *Static and dynamic properties of injection-locked semiconductor lasers*, IEEE J. of Quantum Electronics, Vol 30 (1994), No 8, pp 1701-1708.

20. Mogensen, F. and H. Olesen, G. Jacobsen, *Locking conditions and stability properties for a semiconductor laser with external light injection*, IEEE J. of Quantum Electronics, Vol QE-21 (1985), No 7, pp 784-793.

21. Debernardi, P., *Locking characteristics of Fabry-Perot semiconductor laser oscillators with side-mode injection*, Optics Letters, Vol 21 (1996), No 9, pp 656-658.

22. Iida, Y. and T. Miyajima, M. Morita, *Locking characteristics of intermodal injection locking for a semiconductor laser*, Electronics and Communications in Japan, Part 2, Vol 76 (1993), No 4, pp 22-31.

23. Luo, J.-M. and M. Osinski, *Stable-locking bandwith in sidemode injection locked semiconductor lasers*, Electronics Letters, Vol 27 (1991), No 19, pp 1737-1739.

24. Goldberg, L. and H.F. Taylor, J.F. Weller, *Intermodal injection locking and gain profile measurement of GaAlAs lasers*, IEEE J. of Quantum Electronics, Vol QE-20 (1984), No 11, pp 1226-1229.

25. Van Tartwijk, G.H.M. and G. Muijers, D. Lenstra, M.P. van Exter, J.P. Woerdman, *The semiconductor laser beyond the locking range of optical injection*, Electronics Letters, Vol 29 (1993), No 2, pp 137-138.

26. Cerboneschi, E. and D. Hennequin, E. Arimondo, *Frequency conversion in external cavity lasers exposed to optical injection*, IEEE J. of Quantum Electronics, Vol QE-32 (1996), No 2, pp 192-200.

27. Nakajima, H. and R. Frey, *Intracavity nearly degenerate four-wave mixing in a (GaAl)As semiconductor laser*, Applied Physics Letters, Vol 47 (1985), No 8, pp 769-771.

28. Provost, J.G. and R. Frey, *Cavity-enhanced highly nondegenerate four-wave mixing in GaAlAs semiconductor lasers*, Applied Physics Letters, Vol 55 (1989), No 6, pp 519-521.

29. Nietzke, R. and P. Panknin, W. Elsässer, E.O. Göbel, *Four-wave mixing in GaAs/AlGaAs semiconductor lasers*, IEEE J. of Quantum Electronics, Vol 25 (1989), No 6, pp 1399-1406.

30. Gade, N. and J.H. Osmundsen, *Gain measurements on semiconductor lasers by optical feedback from an external grating cavity*, IEEE J. of Quantum Electronics, Vol QE-19 (1983), No 8, pp 1238-1242.

31. Littman, M.G. and H.J. Metcalf, *Spectrally narrow pulsed dye laser without beam expander*, Applied Optics, Vol 17 (1978), No 14, pp 2224-2227.

32. Harvey, K.C. and C.J. Myatt, *External-cavity diode laser using a grazing-incidence diffraction grating*, Optics Letters, Vol 16 (1991), No 12, pp 910-912.

Appendix A Equipment

A.1 The optical multichannel analyser

The laser spectra can be measured on a wide wavelength scale with the Optical Multichannel Analyser (OMA). The light, coupled out of the experimental setup, is lead to the OMA by way of a fibre. First, the light is first coupled into a monochromator. In this monochromator, the light is diffracted by a grating. The diffracted light is projected on a CCD-camera. This CCD-camera consists of linear pixel array. When illuminated, each pixel takes on a value, proportional to the optical power illuminating that pixel. Each different pixel represents a different wavelength. The OMA shows the spectrum by displaying the value of each pixel. The used OMA, the EG&G Princeton Applied Research model 1460, has 1024 pixels, spanning a wavelength range of approximately 26,5 nm, from 666 nm to 692.5 nm.

A.2 The spectrum analyser

The spectra can also be measured on a narrow wavelength scale with a spectrum analyser. It consists of a Fabry-Perot etalon and a controller. Such an etalon consists of 2 mirrors with a very high reflectivity. As in a Fabry-Perot laser cavity (see section 2.2) only discrete frequencies can be transmitted, dependent on the mirror separation. One of the mirrors is mounted on a piezo-element, which makes it possible to change the etalon cavity length. The very narrow transmission peak is shifted over the spectrum of the incoming light. The transmitted light is measured with a detector. The output of this detector can be displayed on an oscilloscope as function of the piezo-voltage, applied on the etalon mirror. In this way, the spectrum of the incoming light is obtained. The separation of the 2 mirrors determines the free spectral range of the etalon, comparable to the mode spacing in the FP-laser cavity. The resolution is determined by the width of the transmission peak. The etalon, used in this report, has a free spectral range of 1,5 GHz (corresponds with approximately 0,0023 nm) and a resolution of about 7 MHz.

A.3 Detectors

The optical power of a light ray can be measured with a detector. The output of such a detector is a voltage. The detector is linear in only a limited part of its range. Hence, it is necessary to determine a calibration curve with a calibrated detector. The calibration curve for the detector, used in the experiments, described in this thesis, is shown in Figure A-1.

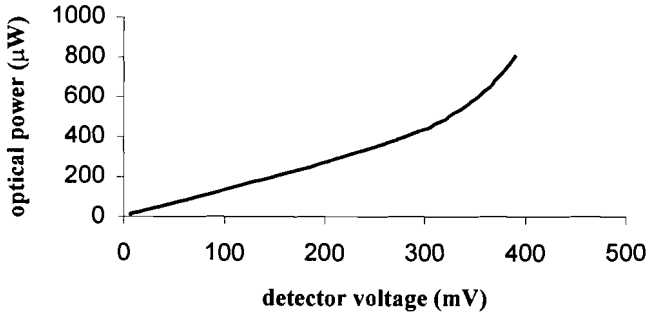

Figure A-1: Detector calibration curve

For the linear part of the detector range, the power can be approximated by the relation:

$$P = 1{,}33 * V + 2{,}31, \qquad \text{(A.1)}$$

with P the optical power in μW and V the measured voltage in mV.
With this equation, each measured voltage can be expressed in an optical power. The optical power, coupled into the detector, is strongly dependent of the cavity setup and alignment. Each time the setup or alignment is changed, the detector must be properly calibrated.

A.4 The liquid crystal displays

In the experimental setup, 2 LCD's are used. In Figure A-2, the transmission curve of the LCD, placed in the external cavity of the neuron laser is shown (see section 5.2). The transmission is taken relative to the maximal transmission. In the experiments, the region from approximately 4V to 6V is used. This is done because in this region, the most grey-scales are available.

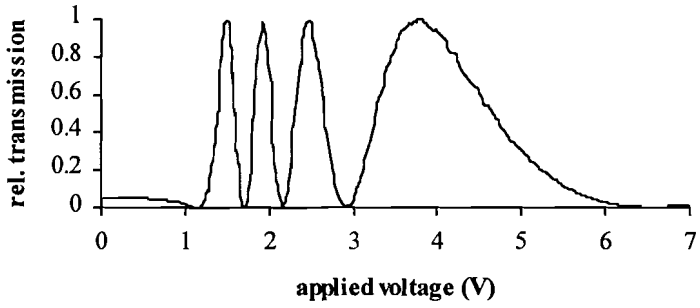

Figure A-2: Transmission of the neuron laser LCD

The light, coming from the tunable lasers is amplitude modulated by a combination of a λ/2 plate, a polariser and a LCD (see section 5.3). The transmission of this combination is shown in Figure A-3.

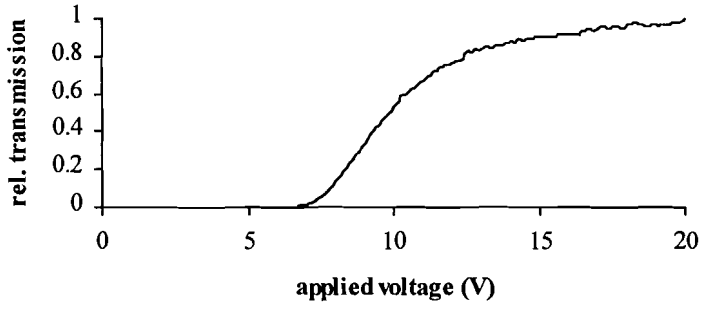

Figure A-3: Transmission of the tunable laser LCD

In both Figures, the applied voltage is the effective voltage.